Zoologischer Anzeiger
September 2019, Volume 282, Pages 140-160
https://doi.org/10.1016/j.jcz.2019.05.011
https://archimer.ifremer.fr/doc/00501/61246/

Four new species of Kinorhyncha from the Gulf of California, eastern Pacific Ocean

Cepeda Diego [1, *], Álvarez-Castillo Lucia [2], Hermoso-Salazar Margarita [2], Sanchez Nuria [1, 3], Gomez Samuel [4], Pardos Fernando [1]

[1] Departamento de Biodiversidad, Ecología y Evolución, Facultad de Ciencias, Biológicas, Universidad Complutense de Madrid. José Antonio Novais St. 12. 28040 Madrid (Spain)
[2] Facultad de Ciencias, Universidad Nacional Autónoma de México. Circuito Exterior S/N, 04510 México, D.F., Mexico
[3] Laboratoire Environnement Profond, Institut Français de Recherche pour, l'Exploitation de la Mer (IFREMER), Centre Bretagne - ZI de la Pointe du Diable, CS 10070 - 29280 Plouzané (France)
[4] Universidad Nacional Autónoma de México, Instituto de Ciencias del Mar y Limnología, Unidad Académica de Mazatlán. Cap. Joel Montes Camarena, Cerro del Vigía. 82040 Mazatlán, Sin., Mexico

* Corresponding author : Diego Cepeda, email address : diegocepeda@ucm.es

Abstract :

Several meiofaunal samples from the central and lower Gulf of California were studied. Four new species of kinorhynchs, Cristaphyes fortis sp. nov., Higginsium mazatlanensis sp. nov., Cephalorhyncha teresae sp. nov. and Echinoderes xalkutaat sp. nov., are described herein. Cristaphyes fortis sp. nov. may be distinguished from its most similar congeners by its more strongly developed pachycycli and ball-and-socket joints and the presence of unpaired paradorsal setae on segments 2, 4 and 6, two pairs of ventrolateral setae on segment 5, one pair of ventrolateral setae on segments 2–4, 6–7 and 10, and one pair of ventromedial setae on segments 8–9. Higginsium mazatlanensis sp. nov. is easily distinguished from its congeners by the combined presence of subdorsal setae only on segment 1 and lateroventral setae only on even segments. Cephalorhyncha teresae sp. nov. is unique within the genus by the presence of acicular spines in middorsal position on segments 4, 6 and 8, in sublateral position on segment 7 and in lateroventral position on segments 8 and 9, as well as tubes in subdorsal position on segment 2, and in lateroventral position on segment 5. Moreover, this species has primary pectinate fringes of segments 2–7 bearing a tuft of elongated spinous projections in middorsal position, which is unique among its congeners. Echinoderes xalkutaat sp. nov. belongs to a group of Echinoderes characterized by possessing type 2 glandular cell outlets in subdorsal, laterodorsal, sublateral and ventrolateral positions on segment 2, together with middorsal spines on segments 4–8, lateroventral spines on segments 6–9 and lateroventral tubes on segment 5, but the arrangement of the remaining type 2 glandular cell outlets (in midlateral position on segment 5, in sublateral position on segment 8 and in laterodorsal position on segment 10) and the cuticular composition of segment 11 (one tergal and two sternal plates) allow its morphological differentiation.

Keywords : Kinorhynchs, meiofauna, biodiversity, taxonomy, Pycnophyidae, Echinoderidae

1. Introduction

Kinorhynchs, commonly known as mud dragons, are marine, holobenthic, meiofaunal invertebrates that inhabit the upper centimetres of the bottom sea sediments (Neuhaus, 2013; Sørensen and Pardos, 2008). Species of kinorhynchs are distributed worldwide, and can be found from shallow waters to the deep sea (Neuhaus, 2013). Despite the apparent ubiquity of the phylum, only a few regions have been extensively sampled, and little is known about the true diversity and biogeography of these invertebrates (Grzelak and Sørensen, 2018; Neuhaus, 2013). Meiofaunal organisms are essential for the functioning of marine food webs and ecosystem (Gerlach, 1971; Hakenkamp and Morin, 2001; Schmid-Araya et al. 2002; Schratzberger and Ingels, 2017). The current lack of knowledge that hampers biodiversity estimations of meiofaunal taxa (Appeltans et al. 2012; Mokievsky and Azovsky, 2002) leads to the need of further taxonomic studies in order to improve our understanding of meiofaunal marine communities.

The Gulf of California represents an important gap in our knowledge on the distribution of Kinorhyncha from the eastern Pacific. The upper gulf has been recently studied by Álvarez-Castillo et al. (2015; 2018). They reported the kinorhynch *Fissuroderes thermoi* Neuhaus and Blasche, 2006 and the presence of ten additional unidentified kinorhynch species of the genus *Echinoderes* and the family Pycnophyidae. However, the central and lower gulf has received little attention, and the kinorhynch species composition of this part of the Gulf remains unexplored. The present contribution increases our knowledge on the diversity of Kinorhyncha in the central and lower Gulf of California with the description of two new Pycnophyidae and two new Echinoderidae species.

2. Material and methods

Sediment samples were collected at two localities in the central Gulf of California and one locality off Mazatlán, Sinaloa State, northwestern Mexico, lower gulf (Fig. 1; Table 1).

Samples from the central gulf were collected on February 11, 2007 during the course of oceanographic cruise Talud X on board of R/V El Puma (Universidad

Nacional Autónoma de México). A sediment sample was collected at each station using a box corer, from which three replicas were taken using an acrylic corer of 9.2 cm of internal diameter and 19.5 cm long. The upper 3 cm layer of the sediment was recovered and preserved in 96% ethanol. Specimens of Kinorhyncha were firstly separated from the sediment particles and remaining meiofaunal organisms. Sample "St15" is located at 1570 m depth and the sediment was mainly composed of mud (sand: 4.49%, silt: 84.00%, clay: 11.96%) with a low content of organic matter (8.37%). Sample "St18" is located at 1440 m depth and the sediment was also composed of mud (sand: 17.20%, silt: 71.62%, clay: 11.19%) with a low content of organic matter too (7.13%).

The sediment sample from Mazatlán was taken at a sampling station located about 8.7 km south of Mazatlán on May 18, 2018 (sample "L3"). The sample was taken with a meiobenthic dredge during the Workshop "Técnicas de muestreo, morfología, taxonomía y análisis genético en meiofauna: Copépodos harpacticoides (Crustacea, Copepoda) y Kinorrincos (Cephalorhyncha, Kinorhyncha) como modelos", that took place at the Instituto de Ciencias del Mar y Limnología at Mazatlán. Sample "L3" is located at 5 m depth and the sediment was mainly composed of sandy mud. Meiofaunal organisms were separated from the sediment using the bubble-and-blot method (Higgins, 1964), and kinorhynchs were preserved in 100% ethanol.

All the studied kinorhynch specimens were picked up under a Motic® SMZ-168 stereo zoom microscope with an Irwin loop and treated with a series of 25%, 50%, 75% and 100% glycerin for light microscopy (LM). The specimens were mounted on glass slides with Fluoromount G® sealed with Depex®. The specimens were studied and photographed using an Olympus® BX51-P microscope equipped with differential interference contrast (DIC) and an Olympus® DP-70 camera. Measurements were obtained with Olympus cellSens® software. Line drawings and image plates were prepared with Adobe® Photoshop CC-2014 and Illustrator CC-2014 software.

The type material was deposited in the collection of the Smithsonian National Museum of Natural History (NMNH), Washington.

3. Results and discussion

Taxonomic account

Class Allomalorhagida Sørensen et al., 2015

Family Pycnophyidae Zelinka, 1896

Genus *Cristaphyes* Sánchez et al., 2016

3.1 *Cristaphyes fortis* sp. nov.

(Figs. 2–5 and Tables 2–3)

urn:lsid:zoobank.org:act:1909D377-717B-4708-AA5F-176EA50569F8

3.1.1 Type material

Adult male holotype (USNM 1558492) collected on February 11, 2007 in the central Gulf of California, eastern Pacific (St15): 27º42´00´´N, 111º38´00´´W; 1570 m depth; mounted in Fluoromount G®. One adult male paratype (USNM 1558494) with same collecting data as holotype, and two adult females paratypes (USNM 1558495-1558496) collected on February 12, 2007 in the central Gulf of California, eastern Pacific (St18): 27º09´08´´N, 111º39´57´´W; 1440 m depth; mounted in Fluoromount G®.

3.1.2 Diagnosis

Cristaphyes with middorsal processes on segments 2–10; process of segment 10 shorter and thinner than previous ones. Unpaired paradorsal setae on segments 2, 4 and 6. Paralateral seta on segment 1; laterodorsal setae on segments 2–9, although those of segments 5–7 and 9 may be absent or only present on one side; lateroventral setae on segments 2, 4, 6, 8 and 10; two pairs of ventrolateral setae on segment 5 and one pair on segments 2–4, 6–7 and 10; paired ventromedial setae on segments 8–9. Pachycycli and ball-and-socket joints strongly developed, thick and stout, distinctly visible on segments 2–10.

3.1.3 Etymology

The specific epithet from the Latin "*fortis*", strong or stout, refers to the markedly thick, robust pachycycli and ball-and-socket joints of the new species.

3.1.4 Description

147 See Table 2 for measurements and dimensions, and Table 3 for summary of location of
148 cuticular processes, setae, glandular cell outlets, spines, nephridiopores and sensory
149 spots.

150 Head with retractable mouth cone and introvert (Fig. 3A-E). Although all the
151 examined specimens had the introvert completely everted, oral styles and scalids tended
152 to collapse when mounted for LM. There were no specimens for SEM examination, and
153 only some details of the head structures are given. Observed inner oral styles composed
154 of a single unit with a trapezoidal, enlarged base and a triangular, straight, rigid distal
155 tip (Fig. 3C). Following ring (ring 00) with nine outer oral styles (Fig. 3D). Outer oral
156 styles composed of a single, very flexible piece with a basal, short, fringed sheath (Fig.
157 3D-E). Exact arrangement and detailed morphology of these oral styles not determined.
158 Ring 01 of introvert with ten primary spinoscalids, each one composed of a basal sheath
159 and a distal, elongated piece; basal sheath equipped with a median, dense fringe (Fig.
160 3E). Remaining rings of introvert (rings 02-06) with scalids morphologically similar to
161 the primary spinoscalids but shorter (Fig. 3E). Fourteen elongated, hairy trichoscalids
162 without trichoscalid plates (Fig. 3E). Exact number, arrangement and detailed
163 morphology of scalids not determined.

164 Neck with four dorsal and two ventral sclerotized placids (Fig. 2A-B). Dorsal
165 placids rectangular; mesial ones broader than lateral ones (Fig. 2B). Ventral placids
166 much more elongated and trapezoidal, progressively thinner laterally (Fig. 2A).

167 Trunk markedly rectangular, stout, strongly sclerotized, triangular in cross-
168 section, composed of eleven segments (Figs. 2A-B and 3A-B). Segment 1 with one
169 tergal, two episternal and one trapezoidal, midsternal plate conspicuously broader at its
170 base (Figs. 2A-B and 3A-B); remaining segments with one tergal and two sternal,
171 cuticular plates (Figs. 2A-B and 3A-B). Sternal plates reach their maximum width at
172 segment 5, but are almost constant in width throughout the trunk, slightly tapering at the
173 posterior trunk end (Figs. 2A-B and 3A-B). Middorsal processes on segments 2–10,
174 keel-shaped, with enlarged, pointed tips that reach one quarter of the total length of the
175 following plate on most segments; middorsal processes increase in width and length
176 segment by segment towards the posterior trunk end (Figs. 2B and 3A); middorsal
177 process of segment 10 shorter and thinner than previous ones (Figs. 2B and 5I).
178 Segments 1–10 with paired glandular cell outlets in subdorsal and ventromedial
179 positions (ventromedial ones of segment 1 laterally shifted to ventrolateral position),

near the anterior margin of segments, circular to oval-shaped (Figs. 2A-B, 4A-J and 5A-J). Segments 2–10 with paired, poorly-marked cuticular ridges in laterodorsal position and also at the ventrolateral-ventromedial limit, next to small glandular cell outlets (Fig. 2A-B, 4D, F, H, J and 5H, J). Muscular scars conspicuous, smooth, hairless, rounded to oval-shaped, in laterodorsal and ventromedial positions on segments 1–10 (except for the ventral muscular scars of segment 1 that are ventrolateral) (Figs. 2A-B, 4A-J and 5A-J). Pachycycli and ball-and-socket joints well-developed, thick, on segments 2–10 (Figs. 2A-B and 3A-B). Apodemes not observed. Posterior margin of segments straight, showing well-developed primary pectinate fringes weakly serrated; secondary pectinate fringes not detectable under LM (Fig. 2A-B).

Segment 1 without middorsal process (Figs. 2B and 3A). Anterolateral margins of the tergal plate as horn-shaped, straight, distally rounded extensions (Figs. 2A-B and 3A). Anterior margin of tergal plate strongly denticulated, followed by paired longitudinal grooves in subdorsal position (Figs. 2B and 4A). Paired setae in paralateral position (Figs. 2B and 4A). Paired sensory spots in laterodorsal and ventrolateral positions, distributed on the anterior half of segment, the former near the paralateral setae, the latter near the ventrolateral glandular cell outlets (Figs. 2A-B and 4A-B). Detailed morphology of sensory spots not determined.

Segment 2 with middorsal process projecting beyond the posterior margin of segment (Figs. 2B and 4C). Unpaired seta in paradorsal position (Figs. 2B and 4C); and paired setae in laterodorsal, lateroventral and ventrolateral positions (Figs. 2A-B and 4C-D). Two pairs of sensory spots in subdorsal position, one posterior to the subdorsal glandular cell outlets, the other mesial to muscular scars (Figs. 2B and 4C); and one pair of sensory spots in laterodorsal position (Figs. 2B and 4C). Sternal plates with two pairs of sensory spots in ventromedial position, lateral to the ventral muscular scars (Figs. 2A and 4D). Sexually dimorphic male tubes absent (Fig. 2A).

Segment 3 with middorsal process as on the preceding segment (Figs. 2B and 4E). Paired setae in laterodorsal and ventrolateral positions (Figs. 2A-B and 4E-F). Paired sensory spots in subdorsal, laterodorsal and ventromedial positions, with the laterodorsal pair lateral to the setae (Figs. 2A-B and 4E-F).

Segment 4 with middorsal process as on the preceding segment (Figs. 2B and 4G). Unpaired seta in paradorsal position (Figs. 2B and 4G); paired setae in

212 laterodorsal, lateroventral and ventrolateral positions (Figs. 2A-B and 4G-H). Paired
213 sensory spots in subdorsal, laterodorsal and ventromedial positions, with the
214 laterodorsal pair lateral to the setae (Figs. 2A-B and 4G-H).

215 Segment 5 with middorsal process as on the preceding segment (Figs. 2B and
216 4I). One pair of setae in laterodorsal position (Figs. 2B and 4I), and two pairs of setae in
217 ventrolateral position (Figs. 2A and 4J). Laterodorsal setae with intraspecific variation,
218 absent in some specimens or present only on one side of the tergal plate. Paired sensory
219 spots in subdorsal, laterodorsal and ventromedial positions, with the laterodorsal pair
220 lateral to the setae (Figs. 2A-B and 4I-J).

221 Segment 6 similar to segment 4 in the arrangement of cuticular process, setae
222 and sensory spots (Figs. 2A-B and 5A-B). Laterodorsal setae on this segment showing
223 intraspecific variation as those of segment 5.

224 Segment 7 similar to segment 5 in the arrangement of cuticular process, setae
225 and sensory spots, except for the presence of a single pair of ventrolateral setae (Figs.
226 2A-B and 5C-D).

227 Segment 8 with middorsal process as on the preceding segment (Figs. 2B and
228 5E). Paired setae in laterodorsal, lateroventral and ventromedial positions (Figs. 2A-B
229 and 5E-F). Paired sensory spots in subdorsal, laterodorsal and ventromedial positions,
230 the latter mesial to ventromedial setae (Figs. 2A-B and 5E-F).

231 Segment 9 with middorsal process as on the preceding segment (Figs. 2B and
232 5G). Paired setae in laterodorsal and ventromedial positions (Figs. 2A-B and 5G-H).
233 Laterodorsal setae with intraspecific variability, as those of segment 5. Paired sensory
234 spots in subdorsal, laterodorsal and ventromedial positions (Figs. 2A-B and 5G-H), the
235 latter lateral or mesial to the ventromedial setae. Paired nephridiopores in paralateral
236 position; detailed morphology of nephridiopores not determined.

237 Segment 10 with short middorsal process, less developed than in previous
238 segments (Figs. 2B and 5I). Paired setae in lateroventral and ventrolateral positions
239 (Figs. 2A-B and 5J). Paired sensory spots in subdorsal and laterodorsal positions, near
240 the posterior margin of segment (Figs. 2B and 5I).

241 Segment 11 with paired type 3 sensory spots in subdorsal and laterodorsal
242 positions (Figs. 2B and 5K). Males with two pairs of stout, thick, penile spines and

genital pores surrounded by a tuft of long hairs (Figs. 2A-B and 5L). Lateral terminal spines long (LTS:TL average ratio = 29.0%), slender, narrow, apparently rigid, with rounded tips (Figs. 2A-B and 3A-B, F).

3.1.5 Remarks on differential characters

This species clearly belongs to the genus *Cristaphyes* by the following diagnostic features: middorsal processes on segments 2–10, surpassing the posterior margin of segments, progressively longer towards segment 9, and well-developed pachycycli and ball-and-socket joints of similar size on segments 2–10 (Sánchez et al. 2016). However, it may be distinguished from the remaining congeners by its unique arrangement of cuticular processes, setae and spines.

Cristaphyes fortis sp. nov. is characterized by having lateral terminal spines on segment 11, and by lacking ventromedial, sexually dimorphic tubes in males, structures that are usually present in the family Pycnophyidae (Sánchez et al. 2016). Only *C. chilensis* (Lang, 1953), *C. cornifrons* Cepeda et al., this issue, *C. longicornis* (Higgins, 1983) and *C. nubilis* (Sánchez et al., 2014), share the combination of missing tubes and possessing lateral terminal spines with the new species. Moreover, *C. fortis* sp. nov., *C. cornifrons* and *C. longicornis* share the arrangement of middorsal processes throughout segments 2–10, whereas the middorsal processes of *C. chilensis* and *C. nubilis* are present from segment 1.

Cristaphyes fortis sp. nov. can be distinguished from *C. cornifrons* and *C. longicornis* by its pattern of setae and spines. *Cristaphyes longicornis* is characterized by having unpaired setae in paradorsal position on segments 2, 4, 6 and 8, whereas *C. fortis* sp. nov. possesses these unpaired paradorsal setae only on segments 2, 4 and 6. Moreover, *C. longicornis* has one pair of ventrolateral setae on segments 2, 5 and 10 and one pair of ventromedial setae on segments 1 and 3–9, while the new species has two pairs of ventrolateral setae on segment 5, one pair of ventrolateral setae on segments 2–4, 6–7 and 10, and one pair of ventromedial setae on segments 8–9. *Cristaphyes cornifrons* is even more similar to *C. fortis* sp. nov. in the arrangement of the tergal setae, but differs remarkably on the sternal ones. Thus, *C. cornifrons* is characterized by having one pair of ventrolateral setae on segments 2–3, 5 and 10 (the last one only in females) and one pair of ventromedial setae on segments 4–9, whereas *C. fortis* sp. nov. has two pairs of ventrolateral setae on segment 5, one pair of

ventrolateral setae on segments 2–4, 6–7 and 10, and one pair of ventromedial setae on segments 8–9.

Genus *Higginsium* Sánchez et al., 2016

3.2 *Higginsium mazatlanensis* sp. nov.

(Figs. 6–9 and Tables 4–5)

urn:lsid:zoobank.org:act:0D79B812-D3CB-4CD9-8EE7-21361DF105A0

3.2.1 Type material

Adult male holotype (USNM 1558497) collected on May 18, 2018 near the mouth of Presidio River, south of Mazatlán, Sinaloa State, Mexico (southern Gulf of California), eastern Pacific (L3): 23º05´30´´N, 106º17´45´´W; 5 m depth; mounted in Fluoromount G®. Two adult males (USNM 1558499-1558500) and one adult female (USNM 1558498) paratypes with same collecting data as holotype; mounted in Fluoromount G®.

3.2.2 Diagnosis

Higginsium with middorsal elevations on segments 1–6, middorsal processes on segments 7–9 and middorsal small pointed projection on segment 10. Anterior margin of first segment with several minute, rounded glandular cell outlets. Unpaired seta in paradorsal position on segments 3, 5, 7 and 9–10; paired setae in paradorsal position on segments 2, 4, 6 and 8. Subdorsal setae on segment 1. Two pairs of laterodorsal setae on segments 2–9, those of even segments more mesial than those of odd segments. Paralateral setae on segment 1. Lateroventral setae on segments 2, 4, 6, 8 and 10 (two pairs on segment 10). Ventromedial setae on segments 2–9. Male with paired, sexually dimorphic ventromedial tubes on segment 2. Lateral terminal spines absent.

3.2.3 Etymology

The name makes refers to the municipality Mazatlán (Sinaloa State, Mexico), where the species was found.

3.2.4 Description

See Table 4 for measurements and dimensions, and Table 5 for summary of location of cuticular elevations, cuticular processes, setae, glandular cell outlets, nephridiopores and sensory spots.

Head with retractable mouth cone and introvert. The collected specimens were not suitable for head examination, hence data on number, morphology and arrangement of scalids and oral styles are not available.

Neck with four dorsal and two ventral sclerotized placids (Figs. 6A-C and 7C-D). Dorsal placids trapezoidal, flattened, with a lateral indentation near the posterior margin; mesial ones broader, not getting narrower towards the lateral sides; lateral ones getting narrower towards the lateral sides, with a concave anterior margin (Figs. 6B and 7C). Ventral placids similar to dorsal mesial ones (Figs. 6A, C and 7D).

Trunk markedly rectangular, stout, sclerotized, triangular in cross-section, composed of eleven segments (Figs. 6A-B and 7A-B). Segment 1 with one tergal, two episternal and one midsternal plate; midsternal plate of segment 1 trapezoidal, laterally extended at its base, with a lateral constriction near its anterior margin, with a straight posterior margin (Figs. 6A-B and 7A-B, D). Remaining trunk segments with one tergal and two sternal plates (Figs. 6A-D and 7A-B). Sternal plates reach their maximum width at segment 6, almost constant in width up to segment 9, progressively tapering towards the posterior end of trunk (Figs. 6A-B and 7A-B). Middorsal elevations on segments 1–6, short, pentagonally-shaped, distally rounded, not projecting beyond the posterior margin of segments, with intracuticular, butterfly-like atria of paradorsal sensory spots (Figs. 6A-B, 7A, 8A, C, E, G, I and 9A). Middorsal processes on segments 7–9, keel-shaped, with enlarged pointed tips, projecting beyond the posterior margin of segments, progressively longer in the last segments (Figs. 6B, 7A and 9C, E, G). Segment 10 also with a small, slightly pointed, very narrow middorsal elevation (Figs. 6B and 9I). Tergal plates of segments 1–10 with paired glandular cell outlets in subdorsal and ventromedial positions (ventral ones of segment 1 in ventrolateral position), near the anterior margin of segments, triangular to crescentic-shaped (Figs. 6A-C, 8A-J and 9A-J). Tergal plates of segments 2–7 with minute, rounded glandular cell outlets in laterodorsal position near the anterior margin of segments (Figs. 6B, 8C, E, G, I and 9A, C). Sternal plates of segments 2–10 with paired cuticular ridges marking the ventrolateral-ventromedial limit, quite inconspicuous on some segments, next to small glandular cell outlets (Figs. 6A, C, 8F, H, J and 9B, D, F, H). Segment 1 with

several, minute, rounded glandular cell outlets, arranged dorsally along an anterior line running parallel to the anterior margin of segment, and ventrally in irregular patches (Figs. 6A-C and 8A-B). Muscular scars smooth, hairless, rounded to oval-shaped, in laterodorsal and ventromedial position on segments 1–10 (Figs. 6A-D, 8A-J and 9A-J). Pachycycli and ball-and-socket joints well-developed in segments 2–10 (Figs. 6A-D and 7A-B). Apodemes only slightly visible between segments 8–9, in paraventral position (Figs. 6A and 7B). Posterior margin of segments straight, with well-developed primary pectinate fringes strongly striated; secondary pectinate fringes developed as three wavy, transverse bands (Figs. 6A-D).

Segment 1 with middorsal elevation not projecting beyond the posterior margin of segment (Figs. 6B and 8A). Anterolateral margins of the tergal plate as horn-shaped, short, narrow, straight, distally pointed extensions (Figs. 6A-C, 7A-B and 8B). Paired setae in subdorsal, paralateral and ventrolateral positions (Figs. 6A-C and 8A-B). Two pairs of sensory spots in subdorsal position; one pair immediately below the subdorsal glandular cell outlets, another pair lateral to the muscular scars (Figs. 6B and 8A). One pair of sensory spots in paradorsal, lateroventral and ventrolateral positions (Figs. 6A-C and 8A-B). Detailed morphology of sensory spots not determined.

Segment 2 with middorsal elevation as on the preceding segment (Figs. 6B and 8C). Two pairs of setae in laterodorsal position, more mesial than those of the following segment, aligned with the remaining laterodorsal pairs of setae of the even segments (Figs. 6B and 8C); one pair of setae in paradorsal, lateroventral, ventrolateral and ventromedial positions (Figs. 6A-C and 8C-D). Paradorsal pair of setae not transversally aligned, so one of the seta appears more anterior than the other (Figs. 6B and 8C). Paired sensory spots in paradorsal, subdorsal, laterodorsal and ventrolateral position (Figs. 6A-C and 8C-D). Sexually dimorphic male tubes in ventromedial position, lateral to the ventromedial glandular cell outlets, short and thick (Figs. 6A and 8D).

Segment 3 with middorsal elevation as on the preceding segment (Figs. 6B and 8E). Unpaired seta in paradorsal position (Figs. 6B and 8E). Two pairs of setae in laterodorsal position, more lateral than those of the preceding segment, aligned with the remaining laterodorsal pairs of setae of the odd segments (Figs. 6B and 8E). One pair of setae in ventrolateral and ventromedial positions (Figs. 6A and 8F). Two pairs of sensory spots in subdorsal position (Figs. 6B and 8E); one pair of sensory spots in paradorsal, laterodorsal and ventromedial position (Figs. 6A-B and 8E-F).

Segment 4 with middorsal elevation as on the preceding segment (Figs. 6B and 8G). Two pairs of setae in laterodorsal position, aligned with the remaining laterodorsal pairs of setae of the even segments (Figs. 6B and 8G); one pair of setae in paradorsal, lateroventral, ventrolateral and ventromedial positions (Figs. 6A-B and 8G-H). Paradorsal pair of setae not transversally aligned, so one of the seta appears more anterior than the other (Figs. 6B and 8G). Two pairs of sensory spots in subdorsal position (Figs. 6B and 8G); one pair of sensory spots in paradorsal, laterodorsal and ventromedial position (Figs. 6A-B and 8G-H).

Segment 5 with middorsal elevation as on the preceding segment (Figs. 6B and 8I). Unpaired seta in paradorsal position, located on the opposite side of that of segment 3 (Figs. 6B and 8I). Two pairs of setae in laterodorsal position, aligned with the remaining laterodorsal pairs of setae of the odd segments, and in ventrolateral position (Figs. 6A-B and 8I-J); one pair of setae in ventromedial position (Figs. 6A and 8J). Two pairs of sensory spots in subdorsal position (Figs. 6B and 8I); one pair of sensory spots in paradorsal, laterodorsal and ventromedial position (Figs. 6A-B and 8I-J).

Segment 6 similar to segment 4 regarding the arrangement of cuticular elevation, setae and sensory spots (Figs. 6A-B and 9A-B).

Segment 7 with middorsal process projecting beyond the posterior margin of segment (Figs. 6B and 9C). Unpaired seta in paradorsal position, on the opposite side of that of segment 5 (Figs. 6B and 9C). Two pairs of setae in laterodorsal position, aligned with the remaining laterodorsal pairs of setae of the odd segments (Figs. 6B and 9C); one pair of setae in ventrolateral and ventromedial positions (Figs. 6A and 9D). Two pairs of sensory spots in subdorsal position (Figs. 6B and 9C); one pair of sensory spots in paradorsal, laterodorsal and ventromedial positions (Figs. 6A-B and 9C-D).

Segment 8 with middorsal process as in the preceding segment (Figs. 6B and 9E). Two pairs of setae in laterodorsal position, aligned with the remaining laterodorsal pairs of setae of the even segments (Figs. 6B and 9E); one pair of setae in paradorsal (not transversally arranged), lateroventral, ventrolateral and ventromedial positions (Figs. 6A-B and 9E-F). Three pairs of sensory spots in subdorsal position (Figs. 6B and 9E); one pair of sensory spots in paradorsal, laterodorsal and ventromedial positions (Figs. 6A-B and 9E-F).

Segment 9 with middorsal process as in the preceding segment (Figs. 6B and 9G). Unpaired seta in paradorsal position, on the opposite side of that of segment 7 (Figs. 6B and 9G). Two pairs of setae in laterodorsal position, aligned with the remaining laterodorsal pairs of setae of the odd segments (Figs. 6B and 9G); one pair of setae in ventrolateral and ventromedial positions (Figs. 6A and 9H). Three pairs of sensory spots in subdorsal position (Figs. 6B and 9G); one pair of sensory spots in paradorsal, laterodorsal and ventromedial positions (Figs. 6A-B and 9G-H). Paired nephridiopores in paralateral position; detailed morphology of nephridiopores not determined.

Segment 10 with slightly pointed, narrow middorsal elevation not surpassing the posterior margin of segment (Figs. 6B and 9I). Unpaired seta in paradorsal position, located on the opposite side of that of the preceding segment (Figs. 6B and 9I). Two pairs of setae in lateroventral position (Figs. 6A-B and 9J). Paired sensory spots in subdorsal, laterodorsal and ventromedial positions (Figs. 6A-B and 9I-J).

Segment 11 with paired type 3 sensory spots in subdorsal position, at the anterior half of segment (Figs. 6B and 9K). Posterior margin of segment of tergal plate straight, softly serrated; sternal plates form a pair of ventral extensions rounded distally (Figs. 6A-B, D and 9K-L). Male with two pairs of stout, thick, hairy penile spines (Figs. 6A-B and 9L). Lateral terminal spines absent.

3.2.5 Remarks on differential characters

Higginsium mazatlanensis sp. nov. agrees well with the diagnosis of the genus (Sánchez et al. 2016), which currently encompasses four species: *H. cataphractum* (Higgins, 1961), described from San Juan Archipelago, Washington State (northeastern Pacific); *H. dolichurum* (Sánchez et al., 2011), described from Ares Ria, Spain (northeastern Atlantic), and *H. erismatum* (Higgins, 1983) and *H. trisetosum* (Higgins, 1983), both described from Belize (Caribbean Sea).

Higginsium dolichurum is the species that most differs from *H. mazatlanensis* sp. nov., as lateral terminal spines are present in the former but absent in the latter. Similarly, *H. dolichurum* lacks sexually dimorphic tubes on the male segment 2, which are present in the new species. The remaining species of the genus (*H. cataphractum*, *H. erismatum* and *H. trisetosum*) and *H. mazatlanensis* sp. nov. share the lack of lateral

terminal spines and the presence of sexually dimorphic tubes in ventromedial position on the male segment 2.

The available morphological information of *H. cataphractum* is rather scarce (Higgins, 1961), and several diagnostic traits that would allow to easier distinction of this species from its congeners could not be observed in the re-examination of the type material by Sánchez et al. (2016) because of the bad preservation of the specimens. However, *H. cataphractum* is characterized by having a single pair of laterodorsal setae on segments 2–9 and lateroventral setae on segments 2, 4, 6–8 and 10, while *H. mazatlanensis* sp. nov. has two pairs of laterodorsal setae on segments 2–9, one pair of lateroventral setae on segments 2, 4, 6 and 8 and two pairs on segment 10.

Higginsium erismatum possesses paired, paradorsal setae only on even segments, a single pair of laterodorsal setae on segments 2–9, paired subdorsal setae on segments 2–9, paired ventrolateral setae on segments 1, 5, 7 and 9, whereas *H. mazatlanensis* sp. nov. is characterized by having unpaired paradorsal setae on segments 3, 5, 7 and 9–10, paired paradorsal setae on segments 2, 4, 6 and 8, two pairs of laterodorsal setae on segments 2–9, paired subdorsal setae only on segment 1, paired ventrolateral setae on segments 2–9. Additionally, the arrangement of ventromedial setae of *H. erismatum* is different in both sexes: the females possess these setae on segments 6–9, whereas males have ventromedial setae also on segments 3–5, while both males and females of *H. mazatlanensis* sp. nov. have two pairs on segment 5 and one pair on segments 2–4 and 6–9.

Higginsium trisetosum is the species that resembles *H. mazatlanensis* sp. nov. the most. Both species have two pairs of laterodorsal setae on segments 2–9, midsternal plate of segment 1 with a mushroom-like appearance (due to a lateral constriction near its anterior margin) and secondary pectinate fringes of segments 2–9 composed of three transverse, wavy, softly serrated bands distributed throughout the anterior half of segments. Nevertheless, *H. trisetosum* has subdorsal setae on segments 2–9 and lateroventral setae on segments 1–10, whereas *H. mazatlanensis* sp. nov. has subdorsal setae only on segment 1 and lateroventral setae only on even segments. Moreover, the sternal plates of *H. trisetosum* have ventrolateral setae on segments 1 and 3–9, and ventromedial setae on segment 3–9 (females also on segment 2), while those of *H. mazatlanensis* sp. nov. bear ventrolateral setae on segments 1–9 and ventromedial setae on segments 2–9 (both males and females).

Another morphological feature that allows distinguishing *H. mazatlanensis* sp. nov. from its congeners is the possession of several, minute, rounded glandular cell outlets distributed near the anterior margin of the tergal plate of segment 1 and throughout the surface of the sternal plates of segment 1. These glandular cell outlets are absent in other species of *Higginsium*.

Class Cyclorhagida (Zelinka, 1896) Sørensen et al., 2015

Family Echinoderidae Zelinka, 1894

Genus *Cephalorhyncha* Adrianov, 1999 in Adrianov and Malakhov, 1999

3.3 *Cephalorhyncha teresae* sp. nov.

(Figs. 10–12 and Tables 6–7)

urn:lsid:zoobank.org:act:260F18A5-472F-47EE-9EC7-51195C84E66B

3.3.1 Type material

Adult female holotype (USNM 1558501) collected on May 18, 2018 off Mazatlán, Sinaloa State, Mexico, eastern Pacific (L3): 23º05´30´´N, 106º17´45´´W; 5 m depth; mounted in Fluoromount G®. Two adult male (USNM 1558502-1558503) and five adult female (USNM 1558504-1558508) paratypes with same collecting data as holotype; mounted in Fluoromount G®.

3.3.2 Diagnosis

Cephalorhyncha with middorsal, acicular spines on segments 4, 6 and 8, in sublateral position on segment 7, and in lateroventral position on segments 8–9. Tubes present in subdorsal position on segment 2 and in lateroventral position on segment 5. Primary pectinate fringe of segments 2–7 with a tuft of elongated spinous projections in middorsal position, whereas straight and not elongated on the sternal plates. Cuticular hairs generally scarce, distributed in one or two straight rows only in the posterior half of the cuticular plates, absent on segments 1 and 11.

3.3.3 Etymology

The species is dedicated to the dear mother of the first author, who always encouraged and supported him in his biological research.

493 *3.3.4 Description*

494 See Table 6 for measurements and dimensions, and Table 7 for summary of location of
495 spines, tubes, nephridiopores, glandular cell outlets and sensory spots.

496 Head with retractable mouth cone and introvert (Fig. 11A-B, D-E). Although the
497 holotype and two paratypes had the head partially everted, oral styles and scalids tended
498 to collapse when mounted for LM. There were no available specimens for SEM
499 examination, and only some details of these structures can be provided. Internal part of
500 mouth cone with several rings of inner oral styles; exact number, morphology and
501 arrangement of inner oral styles not determined. External part of mouth cone with a ring
502 of 9 outer oral styles (Fig. 11D). Outer oral styles alternate between longer and shorter
503 ones; five long styles appear anterior to the odd-numbered introvert sections, whereas
504 four shorter ones appear anterior to the even-numbered introvert sections, except in the
505 middorsal section 6 where a style is missing (Fig. 11D). Outer oral styles with two
506 jointed subunits, with a rectangular, smooth basis and a triangular, hook-like, curved
507 inwards, distal piece (Fig. 11D).

508 Introvert with several rings of cuticular scalids. Ring 01 with ten primary
509 spinoscalids with of a short, quadrangular basal sheath and a distal, elongated end piece;
510 distal piece thick, rounded in cross-section, smooth, hook-like (Fig. 11E). Remaining
511 rings with several scalids also composed of two jointed subunits (Fig. 11E); detailed
512 morphology and arrangement of these scalids not determined.

513 Neck with sixteen distinct, well-defined, trapezoidal placids, wider at base, with
514 a marked joint between the neck and segment 1 (Figs. 10A-B and 11F-G); midventral
515 one widest (ca. 7 μm wide at base) (Figs. 10A and 11G), remaining ones similar in
516 width (ca. 5 μm wide at base) (Figs. 10A-B and 11F-G). Placids closely situated
517 together at base, separated distally by cuticular folds (Figs. 10A-B and 11F-G). Six
518 trichoscalids attach to the placids of the neck via small, oval trichoscalid plates (Figs.
519 10A-B and 11F-G).

520 Trunk slender, markedly tapered towards hind end, composed of eleven trunk
521 segments (Figs. 10A-B and 11A-B). Segment 1 as closed cuticular ring (Figs. 10A-B,
522 11A-B and 12A-B); segment 2 with one tergal and one sternal cuticular plate (Figs.
523 10A-B, 11A-B, H and 12A-B); remaining ones with one tergal and two sternal cuticular
524 plates (Figs. 10A-B, 11A-B and 12A-F). Sternal plate of segment 2 incompletely

subdivided by an indistinct midventral fissure (Fig. 11H); tergosternal joints well-defined, but joint sites without posteriorly extending projections (Fig. 10A). Tergal anterior plates slightly bulging middorsally; posterior ones more flattened, giving the animal a tapering outline in lateral view. Sternal plates reach their maximum width at segment 6, progressively tapering towards the last trunk segments (Figs. 10A and 11B). Cuticular hairs scarce, distributed in one or two straight, transverse rows on each segment at the posterior half of the cuticular plates, except on segments 1 and 11 where cuticular hairs are absent (except those associated with the sensory spots) (Figs. 10A-B and 12A-F); cuticular hairs relatively long, flexible, emerging from rounded perforation sites (Figs. 12A-F). Most of sensory spots flanked by paired, elongated cuticular hairs (Figs. 10A-B and 12A-F). Posterior margin of segments straight, with well-developed primary pectinate fringes with conspicuously serrated free flaps (Figs. 10A-B and 12A-F); primary pectinate fringes of segments 2–8 forming a middorsal tuft of long, spinous projections (Figs. 10A-B and 12A, C). Secondary pectinate fringes well-developed, slightly extending beyond the limit of the primary pectinate fringes (Figs. 10A-B and 12A-F).

Segment 1 without spines, tubes or cuticular hairs (except those associated with the sensory spots). Unpaired type 1 glandular cell outlet in middorsal position, near the anterior margin of segment (Figs. 10B and 12A). Paired sensory spots in subdorsal, laterodorsal and lateroventral position, flanked by cuticular hairs, except the lateroventral ones (Figs. 10A-B and 12A-B); detailed morphology of these and remaining sensory spots not determined.

Segment 2 with paired large tubes in subdorsal position (Figs. 10B and 12A). Unpaired type 1 glandular cell outlet in middorsal position near the anterior margin of segment (Figs. 10B and 12A). Paired sensory spots in paradorsal and midlateral positions, flanked by cuticular hairs (Figs. 10B and 12A).

Segment 3 without spines or tubes. Unpaired type 1 glandular cell outlet in middorsal position, near the anterior margin of segment (Figs. 10B and 12A). Paired sensory spots in paradorsal, subdorsal and sublateral positions, flanked by cuticular hairs (Figs. 10A-B and 12A-B).

Segment 4 with a middorsal spine slightly exceeding the posterior edge of the following segment (Figs. 10B and 12A). Paired sensory spots in paradorsal and

sublateral positions, the former posterior to the base of the middorsal spine, both laterally flanked by cuticular hairs (Figs. 10A-B and 12A-B).

Segment 5 with paired, thickened, very flexible tubes in lateroventral position (Figs. 10A and 12D). Paired sensory spots in ventrolateral position, near the intersection between the ventrolateral and the ventromedial regions, not flanked by cuticular hairs (Figs. 10A and 12D).

Segment 6 with a middorsal acicular spine exceeding the posterior edge of the following segment, but not reaching the posterior margin of segment 8 (Figs. 10B and 12C). Paired sensory spots in paradorsal and ventrolateral regions, the former posterior to the base of the middorsal spine, the latter aligned with those of the previous segment, without lateral cuticular hairs (Figs. 10A-B and 12C-D).

Segment 7 with paired acicular spines in sublateral position, slightly exceeding the posterior edge of the following segment (Figs. 10A-B and 12D). Paired sensory spots in subdorsal position, flanked by cuticular hairs (Figs. 10B and 12C).

Segment 8 with a middorsal acicular spine exceeding the posterior edge of segment 10 but not reaching the posterior end of trunk, and paired acicular spines in lateroventral position, not reaching the posterior edge of the following segment (Figs. 10A-B and 12C-D). Paired sensory spots in paradorsal position, flanked by cuticular hairs (Figs. 10B and 12C).

Segment 9 with paired acicular spines in lateroventral position, slightly exceeding the posterior edge of the following segment (Figs. 10A and 12F). Unpaired type 1 glandular cell outlet in middorsal position, near the anterior margin of segment (Figs. 10B and 12E). Paired sensory spots in paradorsal and laterodorsal positions, flanked by cuticular hairs (Figs. 10B and 12E). Paired nephridiopores in midlateral position (Figs. 10A and 12F); detailed morphology of nephridiopores not determined.

Segment 10 without spines or tubes. Unpaired type 1 glandular cell outlet in middorsal position, near the anterior margin of segment (Figs. 10B and 12E). Paired sensory spots in subdorsal position near the posterior margin of segment, flanked by cuticular hairs (Figs. 10B and 12E).

Segment 11 with lateral terminal spines long (LTS:TL average ratio = 53.3%), slender, flexible, pointed distally, with a central cavity (Figs. 10A-B and 11C). Males

with three pairs of penile spines; one pair short, rigid and stubby, the other ones longer, pointed and much more flexible (Figs. 10C-D). Females with paired lateral terminal accessory spines, much shorter than lateral terminal ones (LTAS:LTS average ratio = 11.5%) (Figs. 10A-B and 11C). Unpaired type 1 glandular cell outlet in middorsal position, near the anterior margin of segment (Figs. 10B, D and 12E). Paired sensory spots in paradorsal position, flanked by cuticular hairs, near the posterior margin of segment (Figs. 10B, D and 12E). Tergal plate with tergal extensions long and pointed distally (Figs. 10B, D and 12E). Sternal plates with rounded sternal extensions (Figs. 10A, C and 12F).

3.4.6 Remarks on differential characters

Cephalorhyncha teresae sp. nov. agrees well with the diagnosis of the genus (Adrianov and Malakhov, 1999; Neuhaus and Blasche, 2006). With the description of the new species, the genus is currently composed of six species: *C. asiatica* (Adrianov, 1989), *C. liticola* Sørensen, 2008, *C. flosculosa* Yildiz et al., 2016, *C. nybakkeni* (Higgins, 1986), a newly described species from Pacific polymetallic nodules (see Sánchez et al., this issue), and *C. teresae* sp. nov. The former five species are characterized by having middorsal, acicular spines on segments 4–8 as well as lateral spines and/or tubes on segments 5–9. *Cephalorhyncha teresae* sp. nov. possesses middorsal, acicular spines only on segments 4, 6 and 8, and lateral spines on segments 8–9 only. Additionally, the five known species share the presence of paired ventrolateral spines or tubes on segment 2, while *C. teresae* sp. nov. has paired tubes in subdorsal position on this segment. Moreover, *C. teresae* sp. nov. is unique among its congeners in the sublateral position of the spines of segment 6.

Regarding the trunk habitus, *C. teresae* sp. nov. is more similar to *C. asiatica*, with a body outline closer to that of the genus *Echinoderes*, whereas *C. nybakkeni* is a slender species more similar to some species of *Meristoderes*, and *C. flosculosa* and *C. liticola* are characterized by having laterally compressed bodies.

Furthermore, most species of the genus have midventral tufts of elongated, spinous extensions belonging to the primary pectinate fringes on most of the trunk segments, which are absent in the newly described species. However, *C. teresae* sp. nov. is unique also in the middorsal position of these tufts of elongated spinous elongations on segments 2–7.

620

621 Genus *Echinoderes* Claparède, 1863

622 **3.4 *Echinoderes xalkutaat* sp. nov.**

623 (Figs. 13–16 and Tables 8–9)

624 urn:lsid:zoobank.org:act:112843D9-15DE-4013-9C00-C2B2445BD537

625 *3.4.1 Type material*

626 Adult female holotype (USNM 1558509) collected on February 11, 2007 at the central
627 Gulf of California, eastern Pacific (St18): 27º09´08´´N, 111º39´57´´W; 1440 m depth;
628 mounted in Fluoromount G®. Two adult female paratypes (USNM 1558510-1558511)
629 with same collecting data as holotype; mounted in Fluoromount G®.

630 *3.4.2 Diagnosis*

631 *Echinoderes* with middorsal spines on segments 4–8, lateroventral spines on segments
632 6–9, and lateroventral tubes on segment 5. Type 2 glandular cell outlets present in
633 subdorsal, laterodorsal, sublateral and ventrolateral positions on segment 2, in
634 midlateral position on segment 5, in sublateral position on segment 8 and laterodorsal
635 position in segment 10. Segment 11 composed of one tergal and two sternal plates,
636 lacking cuticular hairs but with short, tiny hair-like extensions in paradorsal position.

637 *3.4.3 Etymology*

638 The species is named after the myth of the monster “Xalkutaat” of the Paipai people of
639 Santa Catarina, Baja California. According to the legend, Xalkutaat would be a dragon-
640 like creature endowed with fire faced and defeated by a child called “Pies Ligeros”
641 (meaning Light Feet), who gave fire to humanity.

642 *3.4.4 Description*

643 See Table 8 for measurements and dimensions, and Table 9 for summary of the location
644 of spines, tubes, nephridiopores, glandular cell outlets and sensory spots.

645 Head with retractable mouth cone and introvert (Fig. 14B-D). Although one of
646 the paratypes had the introvert partially everted, oral styles and scalids tended to
647 collapse when mounted for LM. There were no available specimens for SEM
648 examination, and only some details of these structures can be provided. Internal part of

mouth cone with several rings of inner oral styles; exact number, arrangement and morphology of inner oral styles not determined. External part of mouth cone with 9 outer oral styles. Outer oral styles alternate between slightly longer and slightly shorter ones (Fig. 14B); five long styles appear anterior to the odd-numbered introvert sections, whereas four sligthly shorter ones appear anterior to the even-numbered introvert sections, except in the middorsal section 6 where a style is missing. Outer oral styles with two jointed subunits, with rectangular basis bearing a short, medial fringe, and a triangular, hook-like, distal structure (Fig. 14B).

Introvert with several rings of scalids. Ring 01 with ten primary spinoscalids with a short, rectangular basal sheath and a distal, long end piece; distal piece wide, rounded to oval in cross-section, smooth, hook-like, with blunt tip (Fig. 14C). Remaining rings with several scalids also composed of two jointed subunits (Fig. 14D); detailed morphology and arrangement of these scalids not determined.

Neck with sixteen trapezoidal placids, wider at base, with a distinct joint between the neck and segment 1 (Figs. 13A-B and 14E); midventral one widest (ca. 12 μm wide at base) (Figs. 13A and 14E), remaining ones alternate between wider and narrower (6–8 μm wide at base) (Figs. 13A-B and 14E). Placids situated closely together at base, separated distally by cuticular folds (Figs. 13A-B and 14E). Six hairy trichoscalids attach to small, longitudinally compressed trichoscalid plates (Figs. 13A-B and 14E).

Trunk markedly slender, distally tapered, composed of eleven trunk segments (Figs. 13A-B and 14A). Segments 1–2 as closed cuticular rings; remaining ones with one tergal and two sternal plates (Figs. 13A-B, 14A, 15A-J and 16A-H). Tergal anterior plates slightly bulging middorsally; posterior ones more flattened, giving the animal a tapering outline in lateral view (Fig. 14A). Sternal plates reach their maximum width at segment 7, progressively tapering towards the last trunk segments (Figs. 13A and 14A). Cuticular hairs densely distributed all over the trunk in irregular, transverse rows increasing in number towards the posterior end of trunk, plus unpaired midventral patches, except the mesial half of sternal plates of segments 3–10, the anterior half of segment 10 and all of segment 11 where cuticular hairs are absent (Figs. 13A-B, 14A, 15A-J and 16A-H). Posterior margin of segments straight, with well-developed primary pectinate fringes that possess elongated, strongly serrated free flaps; secondary pectinate fringes not detected with LM (Fig. 13A-B).

682 Segment 1 without spines or tubes. Unpaired type 1 glandular cell outlet in
683 middorsal position (Figs. 13B and 15A). Paired sensory spots in subdorsal, laterodorsal,
684 sublateral and ventrolateral positions (Figs. 13A-B and 15A-B).

685 Segment 2 without spines or tubes. Unpaired type 1 glandular cell outlet in
686 middorsal position (Figs. 13B and 15C), and paired in ventromedial position (Figs. 13A
687 and 15D). Paired type 2 glandular cell outlets in subdorsal, laterodorsal, sublateral and
688 ventrolateral positions; type 2 glandular cell outlets on this and remaining segments
689 flanked by lateral marginal elongated cuticular hairs (Figs. 13A-B and 15C-D).
690 Unpaired sensory spot in middorsal position, posterior to the middorsal type 1 glandular
691 cell outlet (Figs. 13B and 15C); paired sensory spots in ventromedial position, lateral to
692 the ventromedial type 1 glandular cell outlets, not aligned with those of following
693 segments (Figs. 13A and 15D).

694 Segment 3 without spines or tubes. Unpaired type 1 glandular cell outlet in
695 middorsal position (Figs. 13B and 15E), and paired in ventromedial position (Figs. 13A
696 and 15F). Paired sensory spots in laterodorsal and ventromedial positions, the latter
697 mesial and posterior to the ventromedial type 1 glandular cell outlets (Figs. 13A-B and
698 15E-F).

699 Segment 4 with a middorsal spine exceeding the posterior edge of the following
700 segment (Figs. 13B and 15G). Paired type 1 glandular cell outlets in paradorsal and
701 ventromedial regions (Figs. 13A-B and 15G-H). Paired sensory spots in laterodorsal
702 position (Figs. 13B and 15G).

703 Segment 5 with a middorsal spine exceeding the posterior edge of the following
704 segment, but not reaching the posterior margin of segment 7 (Figs. 13B and 15I), and
705 paired, short, narrow tubes in lateroventral position (Figs. 13A and 15J). Paired type 1
706 glandular cell outlets in paradorsal and ventromedial positions (Figs. 13A-B and 15I-J).
707 Paired type 2 glandular cell outlets in midlateral position (Figs. 13B and 15I). Paired
708 sensory spots in laterodorsal and ventromedial positions, the midlateral pair
709 immediately next to the midlateral type 2 glandular cell outlets and the ventromedial
710 pair posterior to the type 1 glandular cell outlets (Figs. 13A-B and 15I-J).

711 Segment 6 with a middorsal spine exceeding the posterior edge of the following
712 segment but not reaching the posterior margin of segment 8, and paired spines in
713 lateroventral position (Figs. 13A-B and 16A-B). Paired type 1 glandular cell outlets in

paradorsal and ventromedial positions (Figs. 13A-B and 16A-B). Paired sensory spots in paradorsal, subdorsal, laterodorsal, midlateral and ventromedial positions, the paradorsal pair posterior to the paradorsal type 1 glandular cell outlets and the ventromedial pair posterior to the type 1 glandular cell outlets (Figs. 13A-B and 16A-B).

Segment 7 with a middorsal spine exceeding the posterior edge of the following segment but not reaching the posterior margin of segment 9, and paired spines in lateroventral position longer than those of preceding segments (Figs. 13A-B and 16B-C). Paired type 1 glandular cell outlets in paradorsal and ventromedial positions (Figs. 13A-B and 16B-C). Paired sensory spots in paradorsal, laterodorsal, midlateral and ventromedial positions, the paradorsal pair posterior to the paradorsal type 1 glandular cell outlets, the ventromedial pair posterior to the ventromedial type 1 glandular cell outlets (Figs. 13A-B and 16B-C).

Segment 8 with a middorsal spine exceeding the posterior edge of segment 10 but not reaching the posterior end of trunk, and paired spines in lateroventral position longer than those of the preceding segment (Figs. 13A-B and 16B, D). Paired type 1 glandular cell outlets in paradorsal and ventromedial positions (Figs. 13A-B and 16B, D). Paired type 2 glandular cell outlets in sublateral position (Figs. 13A and 16D). Paired sensory spots in paradorsal position, posterior to the paradorsal type 1 glandular cell outlets (Figs. 13B and 16D).

Segment 9 with paired spines in lateroventral position, shorter than those of the preceding segment (Figs. 13A and 16F). Paired type 1 glandular cell outlets in paradorsal and ventromedial positions (Figs. 13A-B and 16E-F). Paired sensory spots in paradorsal, subdorsal, midlateral, sublateral and ventromedial positions (Figs. 13A-B and 16E-F). Nephridiopore as a very small sieve plate, in lateral accessory position (Figs. 13A and 16F).

Segment 10 without spines or tubes. Two unpaired type 1 glandular cell outlets in middorsal position (Figs. 13B and 16G), and paired in ventromedial position (Figs. 13A and 16H). Paired type 2 glandular cell outlets in laterodorsal position, near the posterior margin of segment (Figs. 13B and 16G). Paired sensory spots in subdorsal position (Figs. 13B and 16G).

Segment 11 with lateral terminal spines long (LTS:TL average ratio = 60.6%), slender, flexible, pointed distally, with a central cavity (Figs. 13A-B and 14A). Females with paired lateral accessory terminal spines, shorter than lateral terminal ones (LTAS:LTS average ratio = 18.3%) (Figs. 13A-B and 14A). Unpaired type 1 glandular cell outlet in middorsal position (Figs. 13B and 16G). Paired sensory spots in paradorsal position (Figs. 13B and 16G). Tergal plate of females with small patches bearing short, tiny hair-like extensions in paradorsal position (Fig. 13B). Tergal extensions long, pointed distally; sternal plates distally rounded (Figs. 13A-B and 16I).

3.4.5 Remarks on differential characters

Echinoderes xalkutaat sp. nov. is characterized by possessing middorsal spines on segments 4–8, lateroventral spines on segments 6–9, lateroventral tubes on segment 5, four pairs of type 2 glandular cell outlets on segment 2 and one pair on segments 5, 8 and 10. The general arrangement of spines and tubes in *E. xalkutaat* sp. nov. is one of the most common patterns among species of the genus (Grzelak and Sørensen, 2018; Neuhaus, 2013; Sørensen and Pardos, 2008), but the presence of several pairs of type 2 glandular cell outlets throughout segments 2, 5, 8 and 10 is not as common.

The presence of four pairs of type 2 glandular cell outlets in subdorsal, laterodorsal, sublateral and ventrolateral positions on segment 2, together with the aforementioned arrangement of spines and tubes, is only shared with seven congeners: *E. angustus* Higgins and Kristensen, 1988, *E. cernunnos* Sørensen et al. 2012, *E. drogoni* Grzelak and Sørensen, 2018, *E. juliae* Sørensen et al. 2018, *E. obtuspinosus* Sørensen et al., 2012, *E. romanoi* Landers and Sørensen, 2016 and *E. tubilak* Higgins and Kristensen, 1988. However, the new species possesses paired type 2 glandular cell outlets in midlateral position on segment 5, in sublateral position on segment 8, and in laterodorsal position on segment 10. This combination is only shared with *E. angustus* and *E. drogoni*, whereas *Echinoderes cernunnos* bears these structures on segments 5 and 7–8, *E. juliae* on segments 3–5 and 8, *E. obtuspinosus* on segments 4 and 8, *E. romanoi* on segments 5 and 8 and *E. tubilak* on segments 4–5 and 8 (Grzelak and Sørensen, 2018; Landers and Sørensen, 2016; Sørensen et al. 2012; 2018). *Echinoderes angustus* can be distinguished from the new species by its type 2 glandular cell outlets on segment 4, and *E. drogoni* has the tubes of segment 5 displaced to a lateral accessory position (Grzelak and Sørensen, 2018). Additionally, the female of *E. drogoni* has two

tergal plates on segment 11 (Grzelak and Sørensen, 2018), while that of *E. xalkutaat* sp. nov. possesses only a single tergal plate on segment 11.

4. References

Adrianov, A.V., 1989. The first report on Kinorhyncha of the Sea of Japan. Zool. Zh. 68(7), 17–27.

Adrianov, A.V., Malakhov, V.V., 1999. Cephalorhyncha of the world ocean. KMK Scientific Press, Moscow.

Álvarez-Castillo, L., Hermoso-Salazar, M., Estradas-Romero, A., Prol-Ledesma, R.M., Pardos, F., 2015. First records of Kinorhyncha from the Gulf of California: horizontal and vertical distribution of four genera in shallow basins with CO_2 venting activity. Cah. Biol. Mar. 56(3), 271–281.

Álvarez-Castillo, L., Hermoso-Salazar, M., Estradas-Romero, A., Prol-Ledesma, R.M., Pardos, F., 2018. New record of *Fissuroderes thermoi* (Kinorhyncha: Cyclorhagida) in the Gulf of California. Cah. Biol. Mar. 59, 235–244.

Appeltans, W., Ahyong, S.T., Anderson, G., Angel, M.V., Artois, T., Bailly, N., et al., 2012. The magnitude of global marine species diversity. Curr. Biol. 22, 2189–2202. https://doi.org/10. 1016/j.cub.2012.09.036.

Cepeda, D., Pardos, F., Sánchez, N., this issue. Kinorhyncha from the Caribbean, with the description of two new species from Puerto Rico and Barbados. Zool. Anz., this issue.

Claparède, A.R.E., 1863. Zur Kenntnis der Gattung *Echinoderes* Duj. Beobachtungen über Anatomie und Entwicklungsgeschichte wirbelloser Thiere an der Küste von Normandie angestellt. Verlag von Wilhelm Engelmann, Leipzig.

Gerlach, S.A., 1971. On the importance of marine meiofauna for benthos communities. Oecologia 6, 176–190.

Grzelak, K., Sørensen, M.V., 2018. New species of *Echinoderes* (Kinorhyncha: Cyclorhagida) from Spitsbergen, with additional information about known Arctic species. Mar. Biol. Res. 14, 113–147. https:/doi.org/10.1080/17451000.2017.1367096.

Hakenkamp, C.C., Morin, A., 2001. The importance of meiofauna to lotic ecosystem functioning. Freshwater Biol. 44, 165–175. https://doi.org/10.1046/j.1365-2427.2000.00589.x.

Higgins, R.P., 1961. Three new homalorhage kinorhynchs from the San Juan Archipelago, Washington. J. Elisha Mitchell Sci. Soc. 77(1), 81–88.

Higgins, R.P., 1964. Three new kinorhynchs from the North Carolina Coast. Bull. Mar. Sci. 14, 479–493.

Higgins, R.P., 1983. The Atlantic barrier reef ecosystem at Carrie Bow Cay, Belize, II: Kinorhyncha. Smithson. Contrib. Mar. Sci. 18, 1–131. https://doi.org/10.5479/si.01960768.18.1.

Higgins, R.P., 1986. A new species of *Echinoderes* (Kinorhyncha: Cyclorhagida) from a coarse-sand California beach. Trans. Am. Microsc. Soc. 105, 266–273. https://doi.org/10.2307/3226298.

Higgins, R.P., Kristensen, R.M., 1988. Kinorhyncha from Disko Island, West Greenland. Smithson. Contrib. Zool. 458, 1–55. https://doi.org/10.5479/si.00810282.458.

Landers, S.C., Sørensen, M.V., 2016. Two new species of *Echinoderes* (Kinorhyncha, Cyclorhagida), *E. romanoi* sp n. and *E. joyceae* sp n., from the Gulf of Mexico. ZooKeys 594, 51–71. https://doi.org/10.3897/zookeys.594.8623.

Lang, K., 1953. Reports of the Lund University Chile Expedition 1948-1949. 9. Echinoderida. Lunds Universitets Årsskrift N. F. Avd. 2 49, 3–8.

Mokievsky, V., Azovsky, A., 2002. Re-evaluation of species diversity patterns of free-living marine nematodes. Mar. Ecol. Prog.Ser. 238, 101–108. https://doi.org/10.3354/meps238101.

Neuhaus, B., 2013. Kinorhyncha (=Echinodera), in: Schmidt-Rhaesa, A. (Ed.), Handbook of Zoology, Gastrotricha, Cycloneuralia and Gnathifera, Volume 1 Nematomorpha, Priapulida, Kinorhyncha, Loricifera. De Gruyter, Hamburg, pp. 181–350.

Neuhaus, B., Blasche, T., 2006. *Fissuroderes*, a new genus of Kinorhyncha (Cyclorhagida) from the deep sea and continental shelf of New Zealand and from the

836 continental shelf of Costa Rica. Zool. Anz. 245, 19–52.
837 https://doi.org/10.1016/j.jcz.2006.03.003.

838 Sánchez, N., Pardos, F., Herranz, M., Benito, J., 2011. *Pycnophyes dolichurus* sp. nov.
839 and *P. aulacodes* sp. nov. (Kinorhyncha, Homalorhagida, Pycnophyidae), two new
840 kinorhynchs from Spain with a reevaluation of homalorhagid taxonomic characters.
841 Helgol. Mar. Res. 65, 319–334. https://doi.org/10.1007/s10152-010-0226-z.

842 Sánchez, N., Pardos, F., Martínez-Arbizu, P., this issue. Deep-sea Kinorhyncha
843 diversity of the polymetallic nodule fields at the Clarion-Clipperton Fracture Zone
844 (CCZ). Zool. Anz., this issue.

845 Sánchez, N., Pardos, F., Sørensen, M.V., 2014. Deep-sea Kinorhyncha: two new species
846 from the Guinea Basin, with evaluation of an unusual male feature. Org. Divers. Evol.
847 14(4), 349–361. https://doi.org/10.1007/s13127-014-0182-6.

848 Sánchez, N., Yamasaki, H., Pardos, F., Sørensen, M.V., Martínez, A., 2016.
849 Morphology disentangles the systematics of a ubiquitous but elusive meiofaunal group
850 (Kinorhyncha: Pycnophyidae). Cladistics 32(5), 479–505.
851 https://doi.org/10.1111/cla.12143.

852 Schmid-Araya, J.M., Hildrew, A.G., Robertson, A., Schmid, P.E., Winterbottom, J.,
853 2002. The importance of meiofauna in food webs: evidence from an acid stream.
854 Ecology 83(5), 1271–1285. https://doi.org/10.2307/3071942.

855 Schratzberger, M., Ingels, J., 2017. Meiofauna matters: the roles of meiofauna in
856 benthic ecosystems. J. Exp. Mar. Biol. Ecol. 502, 12–25.
857 https://doi.org/10.1016/j.jembe.2017.01.007.

858 Sørensen, M.V., 2008. A new kinorhynch genus from the Antarctic deep sea and a new
859 species of *Cephalorhyncha* from Hawaii (Kinorhyncha: Cyclorhagida: Echinoderidae).
860 Org. Divers. Evol. 8, 230–232. https://doi.org/10.1016/j.ode.2007.11.003.

861 Sørensen, M.V., Dal Zotto, M., Rho, H.S., Herranz, M., Sánchez, N., Pardos, F.,
862 Yamasaki, H., 2015. Phylogeny of Kinorhyncha based on morphology and two
863 molecular loci. PLoS ONE 10(7), e0133440.
864 https://doi.org/10.1371/journal.pone.0133440.

865 Sørensen, M.V., Pardos, F., 2008. Kinorhynch systematics and biology – An
866 introduction to the study of kinorhynchs, inclusive identification keys to the genera.
867 Meiofauna Marina 16, 21–73.

868 Sørensen, M.V., Rho, H.S., Min, W.G., Kim, D., Chang, C.Y., 2012. An exploration of
869 *Echinoderes* (Kinorhyncha: Cyclorhagida) in Korean and neighboring waters, with the
870 description of four new species and a redescription of *E. tchefouensis* Lou, 1934.
871 Zootaxa 3368, 161–196.

872 Sørensen, M.V., Rohal, M., Thistle, D., 2018. Deep-sea Echinoderidae (Kinorhyncha:
873 Cyclorhagida) from the Northwest Pacific. Eur. J. Taxon. 456, 1–75.
874 https://doi.org/10.5852/ejt.2018.456.

875 Yildiz, N.O., Sørensen, M.V., Karaytug, S., 2016. A new species of *Cephalorhyncha*
876 Adrianov, 1999 (Kinorhyncha: Cyclorhagida) from the Aegean Coast of Turkey.
877 Helgol. Mar. Res. 70, 24. https://doi.org/10.1186/s10152-016-0476-5.

878 Zelinka, C., 1894. Über die Organisation von *Echinoderes*. Verh. Dtsch. Zool. Ges. 4,
879 46–49.

880 Zelinka, C., 1896. Demonstration der Tafeln der *Echinoderes* – Monographie. Verh.
881 Dtsch. Zool. Ges. 6, 197–199.

882

883 FUNDING SOURCES

884 The present study was partially funded by the projects IN-217306-3 and IN-202116, by
885 Programa de Apoyo a Proyectos de Investigación e Innovación Tecnológica (PAPIIT)
886 of Dirección General de Asuntos del Personal Académico (DGAPA); and the project
887 BIO03/2017, granted by Unión Iberoamericana de Universidades (UIU).

888 Cepeda was supported by a predoctoral fellowship of the Universidad
889 Complutense de Madrid UCM (CT27/16-CT28-16).

890

891

892 TABLES

893 Table 1. Data on sampling, localities and collected species.

Location	Geographical coordinates	Sampling date	Habitat	Depth (m)	Sampling method	Collected species
Central Gulf of California (St15)	27º42´00´´N, 111º38´00´´W	11/02/2007	Mud	1570	Box corer	*Cristaphyes fortis* sp.nov.
Central Gulf of California (St18)	27º09´08´´N, 111º39´57´´W	11/02/2007	Mud	1440	Box corer	*Cristaphyes fortis* sp.nov.; *Echinoderes xalkutaat* sp. nov.
South of Mazatlán (L3)	23º05´30´´N, 106º17´45´´W	18/05/2018	Sandy mud	5	Meiobenthic dredge	*Cephalorhyncha teresae* sp. nov.; *Higginsium mazatlanensis* sp. nov.

894

895 Table 2. Measurements of adult *Cristaphyes fortis* sp. nov. from the lower Gulf of
896 California, including number of measured specimens (*n*), mean of data and standard
897 deviation (SD). There were no remarkable differences in size and/or dimension between
898 the two sexes or sampling locations. Abbreviations: LTS, lateral terminal spine; MSW-
899 5, maximum sternal width (on segment 5); S, segment lengths; SW-10, standard sternal
900 width (on segment 10); TL, total length of trunk.

Character	Range	Mean (SD; *n*)
TL (µm)	618.8–664.6	644.5 (19.6; 4)
MSW-5 (µm)	151.6–171.2	159.9 (8.4; 4)
MSW-5/TL (%)	23.9–26.7	24.8 (1.3; 4)
SW-10 (µm)	120.6–134.4	128.8 (5.9; 4)
SW-10/TL (%)	19.5–21.0	20.0 (0.7; 4)
S1 (µm)	94.4–113.3	101.7 (8.5; 4)
S2 (µm)	54.3–67.3	60.8 (7.2; 4)
S3 (µm)	56.3–78.5	65.9 (9.4; 4)
S4 (µm)	62.6–68.0	65.2 (2.4; 4)
S5 (µm)	57.1–75.0	67.5(7.7; 4)
S6 (µm)	65.3–86.6	72.7 (9.5; 4)
S7 (µm)	61.0–77.6	71.2 (7.1; 4)
S8 (µm)	56.7–83.6	69.6 (11.0; 4)
S9 (µm)	69.5–81.5	73.9 (5.5; 4)
S10 (µm)	76.2–86.9	81.3 (5.1; 4)
S11 (µm)	35.0–40.1	37.1 (2.3; 4)
LTS (µm)	173.6–197.4	186.5 (9.9; 4)
LTS/TL (%)	26.6–30.0	29.0 (1.6; 4)

Table 3. Summary of nature and arrangement of sensory spots, glandular cell outlets, cuticular processes, setae, nephridiopores and spines in adults of *Cristaphyes fortis* sp. nov. Abbreviations: cp, cuticular process; gco, glandular cell outlet; LD, laterodorsal; lts, lateral terminal spine; LV, lateroventral; m, male condition of sexually dimorphic character; MD, middorsal; ne, nephridiopore; PD, paradorsal; PL, paralateral; ps, penile spine; SD, subdorsal; se, seta; ss, sensory spot; ss3, type 3 sensory spot; VL, ventrolateral; VM, ventromedial; * indicates intraspecific variation, and that structure may be paired, unpaired or absent; ▲ indicates the presence of unpaired structures.

Segment	MD	PD	SD	LD	PL	LV	VL	VM
1			gco	ss	se		ss, gco	
2	cp	se▲	gco, ssx2	gco, se, ss		se	se, gco	ssx2, gco
3	cp		gco, ss	gco, se, ss			se, gco	ss, gco
4	cp	se▲	gco, ss	gco, se, ss		se	se, gco	ss, gco
5	cp		gco, ss	gco, se*, ss			sex2, gco	ss, gco
6	cp	se▲	gco, ss	gco, se*, ss		se	se, gco	ss, gco
7	cp		gco, ss	gco, se*, ss			se, gco	ss, gco
8	cp		gco, ss	gco, se, ss		se	gco	ss, se, gco
9	cp		gco, ss	gco, se*, ss	ne		gco	ss, se, gco
10	cp		gco, ss	gco, ss		se	se, gco	gco
11			ss3	ss		lts, psx2 (m)		

Table 4. Measurements of adult *Higginsium mazatlanensis* sp. nov. from Mazatlán, including number of measured specimens (*n*), mean of data and standard deviation (SD). There were no remarkable differences in size and/or dimension between the two sexes or sampling locations. Abbreviations: MSW-6, maximum sternal width (on segment 6); S, segment lengths; SW-10, standard sternal width (on segment 10); TL, total length of trunk.

Character	Range	Mean (SD; *n*)
TL (μm)	527.7–581.5	563.9 (25.1; 4)
MSW-6 (μm)	107.5–151.6	133.9 (18.9; 4)
MSW-6/TL (%)	19.0–26.7	23.8 (3.5; 4)
SW-10 (μm)	90.5–104.6	96.7 (7.2; 4)
SW-10/TL (%)	16.0–18.0	17.1 (0.9; 4)
S1 (μm)	60.7–87.9	76.0 (11.3; 4)

S2 (μm)	52.0–57.6	52.6 (6.1; 4)
S3 (μm)	48.4–56.6	54.2 (5.7; 4)
S4 (μm)	53.0–61.4	58.1 (3.7; 4)
S5 (μm)	57.1–64.3	59.2 (3.4; 4)
S6 (μm)	65.4–76.4	68.8 (5.2; 4)
S7 (μm)	62.9–73.1	68.7 (4.3; 4)
S8 (μm)	60.3–84.6	73.3 (11.2; 4)
S9 (μm)	71.4–74.9	73.6 (1.6; 4)
S10 (μm)	39.2–52.7	43.5 (6.2; 4)
S11 (μm)	18.7–26.6	22.8 (3.8; 4)

Table 5. Summary of nature and arrangement of sensory spots, glandular cell outlets, cuticular processes, cuticular elevations, setae, tubes, nephridiopores and spines in adults of *Higginsium mazatlanensis* sp. nov. Abbreviations: ce, cuticular elevation; cp, cuticular process; cpr, cuticular projection; gco, glandular cell outlet; LD, laterodorsal; LV, lateroventral; m, male condition of sexually dimorphic feature; MD, middorsal; ne, nephridiopore; PD, paradorsal; PL, paralateral; ps, penile spine; SD, subdorsal; se, seta; ss, sensory spot; ss3, type 3 sensory spot; tu, tube; VL, ventrolateral; VM, ventromedial; ▲ indicates the presence of unpaired structures.

Segment	**MD**	**PD**	**SD**	**LD**	**PL**	**LV**	**VL**	**VM**
1	ce	ss	gco, se, ssx2	ss	se	ss	se, ss, gco	
2	ce	se, ss	gco, ss	gco, sex2, ss		se	se, ss, gco	se, gco, tu (m)
3	ce	se▲, ss	gco, ssx2	gco, sex2, ss			se, gco	se, ss, gco
4	ce	se, ss	gco, ssx2	gco, sex2, ss		se	se, gco	se, ss, gco
5	ce	se▲, ss	gco, ssx2	gco, sex2, ss			sex2, gco	se, ss, gco
6	ce	se, ss	gco, ssx2	gco, sex2, ss		se	se, gco	se, ss, gco
7	cp	se▲, ss	gco, ssx2	gco, sex2, ss			se, gco	se, ss, gco
8	cp	se, ss	gco, ssx3	sex2, ss		se	se, gco	se, ss, gco
9	cp	se▲, ss	gco, ssx3	sex2, ss	ne		se, gco	se, ss, gco
10	ce	se▲	gco, ss	ss		sex2	gco	ss, gco
11			ss3			psx2 (m)		

927 Table 6. Measurements of adult *Cephalorhyncha teresae* sp. nov. from Mazatlán,
928 including number of measured specimens (*n*), mean of data and standard deviation.
929 Remarkable differences in size and/or dimension between the two sexes were not
930 detected. Abbreviations: ac, acicular spine; LTAS, lateral terminal accessory spine;
931 LTS, lateral terminal spine; LV, lateroventral; MD, middorsal; MSW-6, maximum
932 sternal width (on segment 6); S, segment lengths; SD, subdorsal; SL, sublateral; SW-10,
933 standard sternal width (on segment 10); TL, total length of trunk; tu, tube.

Character	**Range**	**Mean (SD; *n*)**
TL (µm)	178.5–233.4	204.9 (22.1; 8)
MSW-6 (µm)	30.1–40.4	38.5 (5.9; 5)
MSW-6/TL (%)	14.0–17.8	18.2 (4.1; 5)
SW-10 (µm)	14.4–27.6	21.8 (5.3; 5)
SW-10/TL (%)	7.0–14.9	10.3 (3.0; 5)
S1 (µm)	12.6–19.2	16.2 (2.2; 8)
S2 (µm)	15.3–21.9	19.5 (2.2; 8)
S3 (µm)	18.3–24.9	21.9 (2.3; 8)
S4 (µm)	20.0–28.7	23.4 (2.9; 8)
S5 (µm)	22.7–29.5	26.0 (2.7; 8)
S6 (µm)	22.5–32.6	28.1 (3.3; 8)
S7 (µm)	29.9–34.3	32.6 (2.7; 8)
S8 (µm)	28.9–35.7	32.9 (2.6; 8)
S9 (µm)	32.2–35.9	34.0 (1.1; 8)
S10 (µm)	20.9–32.7	28.3 (4.4; 8)
S11 (µm)	20.7–26.2	22.5 (2.0; 8)
SD2 (tu) (µm)	9.6–15.0	13.1 (2.4; 7)
MD4 (ac) (µm)	28.5–40.3	35.0 (4.7; 7)
MD6 (ac) (µm)	40.1–52.7	48.7 (4.2; 7)
MD8 (ac) (µm)	47.2–73.8	63.4 (8.5; 8)
LV5 (tu) (µm)	9.8–27.0	17.2 (5.4; 8)
SL7 (ac) (µm)	37.8–52.4	48.5 (6.1; 7)
LV8 (ac) (µm)	33.4–40.3	37.0 (2.4; 8)
LV9 (ac) (µm)	37.7–42.5	40.1 (1.6; 8)
LTS (µm)	93.4–130.5	110.3 (13.4; 7)
LTAS (µm)	22.1–23.8	23.0 (0.7; 6)
LTS/TL (%)	46.1–64.5	53.3 (3.3; 7)
LTAS/TL (%)	9.5–13.3	11.5 (1.7; 6)
LTAS/LTS (%)	17.0–25.0	20.4 (3.0; 6)

934

Table 7. Summary of nature and arrangement of spines, tubes, sensory spots, glandular cell outlets and nephridiopores in adults of *Cephalorhyncha teresae* sp. nov. Abbreviations: ac, acicular spine; f, female condition of sexually dimorphic character; gco1, type 1 glandular cell outlet; LA, lateral accessory; LD, laterodorsal; ltas, lateral terminal accessory spine; lts, lateral terminal spine; LV, lateroventral; m, male condition of sexually dimorphic character; MD, middorsal; ML, midlateral; ne, nephridiopore; PD, paradorsal; ps, penile spine; SD, subdorsal; SL, sublateral; ss, sensory spot; tu, tube; VL, ventrolateral.

Segment	**MD**	**PD**	**SD**	**LD**	**ML**	**SL**	**LA**	**LV**	**VL**
1	gco1		ss	ss				ss	
2	gco1	ss	tu		ss				
3	gco1	ss	ss			ss			
4	ac	ss				ss			
5								tu	ss
6	ac	ss							ss
7			ss			ac			
8	ac	ss						ac	
9	gco1	ss		ss	ne			ac	
10	gco1		ss						
11	gco1	ss			psx3 (m)		ltas (f)	lts	

Table 8. Measurements of adult *Echinoderes xalkutaat* sp. nov. from the Gulf of California, including number of measured specimens (*n*), mean of data and standard deviation. Remarkable differences in size and/or dimension between the two sexes unknown, as only females were sampled. Abbreviations: ac, acicular spine; LTAS, lateral terminal accessory spine; LTS, lateral terminal spine; LV, lateroventral; MD, middorsal; MSW-7, maximum sternal width (on segment 7); S, segment lengths; SW-10, standard sternal width (on segment 10); TL, total length of trunk; tu, tube.

Character	**Range**	**Mean (SD; *n*)**
TL (µm)	282.2–303.5	290.2 (11.6; 3)
MSW-7 (µm)	48.4–48.9	48.6 (0.4; 2)
MSW-7/TL (%)	17.1–17.2	17.1 (0.0; 2)
SW-10 (µm)	39.7–39.9	39.8 (0.1; 2)
SW-10/TL (%)	13.9–14.1	14.0 (0.1; 2)
S1 (µm)	26.3–29.8	28.0 (1.7; 3)

S2 (μm)	26.1–32.5	29.5 (3.2; 3)
S3 (μm)	30.1–33.9	32.6 (1.5; 3)
S4 (μm)	29.4–33.2	31.9 (2.1; 3)
S5 (μm)	31.3–36.6	34.7 (2.9; 3)
S6 (μm)	35.0–40.8	37.5 (3.0; 3)
S7 (μm)	39.5–42.0	41.0 (1.3; 3)
S8 (μm)	44.5–46.9	45.4 (1.3; 3)
S9 (μm)	40.9–45	42.6 (2.1; 3)
S10 (μm)	34.5–36.7	35.2 (1.2; 3)
S11 (μm)	23.9–31.9	28.6 (4.2; 3)
MD4 (ac) (μm)	41.9–44.3	43.1 (1.7; 2)
MD5 (ac) (μm)	56.0–56.0	56.0 (0.0; 1)
MD6 (ac) (μm)	65.2–74.9	69.1 (5.1; 3)
MD7 (ac) (μm)	70.2–71.5	70.9 (0.6; 3)
MD8 (ac) (μm)	76.6–83.9	79.6 (3.8; 3)
LV5 (tu) (μm)	7.7–10.3	9.1 (1.3; 3)
LV6 (ac) (μm)	28.0–38.2	33.7 (5.2; 3)
LV7 (ac) (μm)	42.1–43.2	42.7 (0.8; 2)
LV8 (ac) (μm)	45.2–47.4	46.5 (1.1; 3)
LV9 (ac) (μm)	32.1–39.3	35.4 (3.7; 3)
LTS (μm)	171.3–178.6	175.9 (4.0; 3)
LTAS (μm)	50.3–56.2	53.1 (3.0; 3)
LTS/TL (%)	58.9–63.0	60.6 (2.1; 3)
LTAS/TL (%)	17.4–19.7	18.3 (1.3; 3)
LTAS/LTS (%)	28.3–32.8	30.2 (2.3; 3)

Table 9. Summary of nature and arrangement of spines, tubes, sensory spots, glandular cell outlets and nephridiopores in adults of *Echinoderes xalkutaat* sp. nov. Abbreviations: ac, acicular spine; f, female condition of sexually dimorphic character; gco1/2, type 1/2 glandular cell outlet; LA, lateral accessory; LD, laterodorsal; ltas, lateral terminal accessory spine; lts, lateral terminal spine; LV, lateroventral; MD, middorsal; ML, midlateral; ne, nephridiopore; PD, paradorsal; SD, subdorsal; SL, sublateral; ss, sensory spot; tu, tube; VL, ventrolateral, VM, ventromedial.

Segment	**MD**	**PD**	**SD**	**LD**	**ML**	**SL**	**LA**	**LV**	**VL**	**VM**
1	gco1		ss	ss		ss			ss	
2	gco1, ss		gco2	gco2		gco2			gco2	gco1, ss
3	gco1			ss						gco1, ss
4	ac	gco1		ss						gco1

5	ac	gco1		ss	gco2			tu	gco1, ss
6	ac	gco1, ss	ss	ss	ss			ac	gco1, ss
7	ac	gco1, ss		ss	ss			ac	gco1, ss
8	ac	gco1, ss				gco2		ac	gco1
9		gco1, ss	ss		ss	ss	ne	ac	gco1, ss
10	gco1, gco1		ss	gco2					gco1
11	gco1	ss					ltas (f)	lts	

FIGURE LEGENDS

Fig. 1. Map showing the sampling locations of the studied kinorhynch specimens in the Gulf of California (Northeast Pacific Ocean).

Fig. 2. Line art illustrations of male *Cristaphyes fortis* sp. nov. (A) Ventral overview of trunk; (B) dorsal overview of trunk. Abbreviations: bsj, ball-and-socket joint; dcr, dorsal cuticular ridge; dpl, dorsal placid; gco, glandular cell outlet; ldms, laterodorsal muscular scar; ldse, laterodorsal seta; ldss, laterodorsal sensory spot; ldss3, laterodorsal type 3 sensory spot; lts, lateral terminal spine; lvse, lateroventral seta; mdp, middorsal process; pc, pachycycli; pdse, paradorsal seta; plse, paralateral seta; ppf, primary pectinate fringe; ps, penile spine; S, segment (number after S indicates the corresponding segment); sdgco, subdorsal glandular cell outlet; sdlg, subdorsal longitudinal groove; sdss, subdorsal sensory spot; sdss3, subdorsal type 3 sensory spot; vcr, ventral cuticular ridge; vlms, ventrolateral muscular scar; vlse, ventrolateral seta; vlss, ventrolateral sensory spot; vmgco, ventromedial glandular cell outlet; vmms,

ventromedial muscular scar; vmse, ventromedial seta; vmss, ventromedial sensory spot; vpl, ventral placid.

Fig. 3. Light micrographs showing trunk overviews and details in the mouth cone, introvert and lateral terminal spines characters of male holotype USNM 1558492 of *Cristaphyes fortis* sp. nov. (A) Dorsal overview of trunk; (B) ventral overview of trunk; (C) mouth cone, detail showing ring -01 of inner oral styles; (D) mouth cone, detail showing outer oral styles; (E) introvert, with detail of the first ring of primary spinoscalids (ring 01), remaining rings of regular scalids, trichoscalids; and horn-like extensions of segment 1; (F) detail of a lateral terminal spine. Abbreviations: bsmc, basal sheath of mouth cone; h, horn-like extension; ios, inner oral style; oos, outer oral style; psc, primary spinoscalid; sc, scalid; ts, trichoscalid.

Fig. 4. Light micrographs showing details of cuticular trunk characters of segments 1–5 of male holotype USNM 1558492 of *Cristaphyes fortis* sp. nov., with main focus on glandular cell outlets, setae, sensory spots and cuticular processes. (A) Left half of tergal plate of segment 1; (B) right half of sternal plates of segment 1; (C) left half of tergal plate of segment 2; (D) right half of sternal plate of segment 2; (E) left half of tergal plate of segment 3; (F) right half of sternal plate of segment 3; (G) left half of tergal plate of segment 4; (H) right half of sternal plate of segment 4; (I) left half of tergal plate of segment 5; (J) right half of sternal plate of segment 5. Abbreviations: ldse, laterodorsal seta; mdp, middorsal process; pdse, paradorsal seta; plse, paralateral seta; sdlg, subdorsal longitudinal groove; vcr, ventral cuticular ridge; vlse, ventrolateral seta; sensory spots are marked as closed circles, and glandular cell outlets as dashed circles; numbers after abbreviation indicate the corresponding segment.

Fig. 5. Light micrographs showing details of cuticular trunk characters of segments 6–11 of male holotype USNM 1558492 of *Cristaphyes fortis* sp. nov., with main focus on glandular cell outlets, setae, sensory spots and cuticular processes. (A) Left half of tergal plate of segment 6; (B) right half of sternal plate of segment 6; (C) left half of tergal plate of segment 7; (D) right half of sternal plate of segment 7; (E) left half of tergal plate of segment 8; (F) right half of sternal plate of segment 8; (G) left half of tergal plate of segment 9; (H) right half of sternal plate of segment 9; (I) left half of tergal plate of segment 10; (J) right half of sternal plate of segment 10; (K) left half of tergal plate of segment 11; (L) right half of sternal plate of segment 11. Abbreviations: ldse, laterodorsal seta; mdp, middorsal process; pdse, paradorsal seta; ps, penile spine;

ss3, type 3 sensory spot; vcr, ventral cuticular ridge; vlse, ventrolateral seta; vmse, ventromedial seta; sensory spots are marked as closed circles, and glandular cell outlets as dashed circles; numbers after abbreviation indicate the corresponding segment.

Fig. 6. Line art illustrations of *Higginsium mazatlanensis* sp. nov. (A) Male, ventral overview of trunk; (B) male, dorsal overview of trunk; (C) female, ventral overview of segments 1–2; (D) female, ventral overview of segments 10–11. Abbreviations: bsj, ball-and-socket joint; dpl, dorsal placid; gco, glandular cell outlet; ia, intracuticular atria; ldms, laterodorsal muscular scar; ldse, laterodorsal seta; ldss, laterodorsal sensory spot; lvse, lateroventral seta; lvss, lateroventral sensory spot; mde, middorsal elevation; mdp, middorsal process; pc, pachycycli; pdse, paradorsal seta; pdss, paradorsal sensory spot; plse, paralateral seta; ppf, primary pectinate fringe; ps, penile spine; pvap, paraventral apodeme; sdgco, subdorsal glandular cell outlet; sdse, subdorsal seta; sdss, subdorsal sensory spot; sdss3, subdorsal type 3 sensory spot; spf, secondary pectinate fringe; vcr, ventral cuticular ridge; vlgco, ventrolateral glandular cell outlet; vlse, ventrolateral seta; vlss, ventrolateral sensory spot; vmgco, ventromedial glandular cell outlet; vmms, ventromedial muscular scar; vmse, ventromedial seta; vmss, ventromedial sensory spot; vmt, ventromedial tube; vpl, ventral placid.

Fig. 7. Light micrographs showing trunk overviews and details in the neck of male holotype USNM 1558497 of *Higginsium mazatlanensis* sp. nov. (A) Dorsal overview of trunk; (B) ventral overview of trunk; (C) dorsal view of neck, with detail in the dorsal placids; (D) ventral view of the neck, with detail in the ventral placids. Abbreviations: dpl, dorsal placid; vpl, ventral placid.

Fig. 8. Light micrographs showing details of cuticular trunk characters of segments 1–5 of male holotype USNM 1558497 of *Higginsium mazatlanensis* sp. nov., with main focus on glandular cell outlets, sensory spots, setae, cuticular elevations and tubes. (A) Left half of tergal plate of segment 1; (B) right half of sternal plates of segment 1; (C) left half of tergal plate of segment 2; (D) right half of sternal plates of segment 2; (E) left half of tergal plate of segment 3; (F) right half of sternal plates of segment 3; (G) left half of tergal plate of segment 4; (H) right half of sternal plates of segment 4; (I) left half of tergal plate of segment 5; (J) right half of sternal plates of segment 5. Abbreviations: ldse, laterodorsal seta; m, male condition of sexually dimorphic character; mde, middorsal elevation; pdse, paradorsal seta; plse, paralateral seta; sdse, subdorsal seta; vlse, ventrolateral seta; vmse, ventromedial seta; vmt, ventromedial

tube; sensory spots are marked as closed circles, and glandular cell outlets as dashed circles; numbers after abbreviation indicate the corresponding segment.

Fig. 9. Light micrographs showing details of cuticular trunk characters of segments 6–11 of male holotype USNM 1558497 of *Higginsium mazatlanensis* sp. nov., with main focus on glandular cell outlets, sensory spots, setae, cuticular elevations and cuticular processes. (A) Left half of tergal plate of segment 6; (B) right half of sternal plates of segment 6; (C) left half of tergal plate of segment 7; (D) right half of sternal plates of segment 7; (E) left half of tergal plate of segment 8; (F) right half of sternal plates of segment 8; (G) left half of tergal plate of segment 9; (H) right half of sternal plates of segment 9; (I) left half of tergal plate of segment 10; (J) right half of tergal and sternal plates of segment 10; (K) left half of tergal plate of segment 11; (L) right half of tergal and sternal plates of segment 11. Abbreviations: ldse, laterodorsal seta; lvse, lateroventral seta; mde, middorsal elevation; mdp, middorsal process; pdse, paradorsal seta; ps, penile spine; ss3, type 3 sensory spot; vlse, ventrolateral seta; vmse, ventromedial seta; sensory spots are marked as closed circles, and glandular cell outlets as dashed circles; numbers after abbreviation indicate the corresponding segment.

Fig. 10. Line art illustrations of *Cephalorhyncha teresae* sp. nov. (A) Ventral overview of female trunk; (B) dorsal overview of female trunk; (C) ventral view of male segments 10–11; (D) dorsal view of male segments 10–11. Abbreviations: dpl, dorsal placid; ldss, laterodorsal sensory spot; ltas, lateral terminal accessory spine; lts, lateral terminal spine; lvs, lateroventral spine; lvss, lateroventral sensory spot; lvt, lateroventral tube; mdgco1, middorsal type 1 glandular cell outlet; mds, middorsal spine; mdtf, middorsal tuft; mlne, midlateral nephridiopore; mlss, midlateral sensory spot; mvpl, midventral placid; pdss, paradorsal sensory spot; ppf, primary pectinate fringe; ps, penile spine; sdss, subdorsal sensory spot; sdt, subdorsal tube; sls, sublateral spine; slss, sublateral sensory spot; spf, secondary pectinate fringe; te, tergal extension; tsp, trichoscalid plate; vlss, ventrolateral sensory spot.

Fig. 11. Light micrographs showing trunk overviews and details in the head, neck, segment 2 and lateral terminal and lateral terminal accessory spines of female holotype USNM 1558501 of *Cephalorhyncha teresae* sp. nov. (A) Dorsal overview of trunk; (B) ventral overview of trunk; (C) ventral view of segment 11, with detail in the lateral terminal and the lateral terminal accessory spines; (D) mouth cone, with detail in the outer oral styles; (E) introvert, with detail in the primary spinoscalids; (F) dorsal view of

neck, with detail in the placids and the trichoscalid plates; (G) ventral view of neck, with detail in the placids; (H) ventral view of segment 2. Abbreviations: ltas, lateral terminal accessory spine; lts, lateral terminal spine; mvp, midventral placid; oos, outer oral style; psc, primary spinoscalid; tsp, trichoscalid plate.

Fig. 12. Light micrographs showing details of cuticular trunk characters of segments 1–11 of female holotype USNM 1558501 of *Cephalorhyncha teresae* sp. nov., with main focus on glandular cell outlets, sensory spots, nephridiopores, tubes and spines. (A) Left half of tergal plate of segments 1-4; (B) right half of sternal plates of segments 1-4; (C) left half of tergal plate of segments 5-8; (D) right half of sternal plates of segments 5-8; (E) left half of tergal plate of segments 9-11; (F) right half of sternal plates of segments 9-11. Abbreviations: lvt, lateroventral tube; lvs, lateroventral spine; mds, middorsal spine; mlne, midlateral nephridiopore; sdt, subdorsal tube; sls, sublateral spine; sensory spots are marked as closed circles, and glandular cell outlets as dashed circles; numbers after abbreviation indicate the corresponding segment.

Fig. 13. Line art illustrations of *Echinoderes xalkutaat* sp. nov. (A) Ventral overview of female trunk; (B) dorsal overview of female trunk. Abbreviations: dpl, dorsal placid; lane, lateral accessory nephridiopore; ldgco2, laterodorsal type 2 glandular cell outlet; ldss, laterodorsal sensory spot; ltas, lateral terminal accessory spine; lts, lateral terminal spine; lvs, lateroventral spine; lvt, lateroventral tube; mdgco1, middorsal type 1 glandular cell outlet; mds, middorsal spine; mdss, middorsal sensory spot; mlgco2, midlateral type 2 glandular cell outlet; mlss, midlateral sensory spot; mvp, midventral placid; pdgco1, paradorsal type 1 glandular cell outlet; pdss, paradorsal sensory spot; ph, patch of hairs; ppf, primary pectinate fringe; sdgco2, subdorsal type 2 glandular cell outlet; sdss, subdorsal sensory spot; slgco2, sublateral type 2 glandular cell outlet; slss, sublateral sensory spot; te, tergal extension; tsp, trichoscalid plate; vlgco2, ventrolateral type 2 glandular cell outlet; vlss, ventrolateral sensory spot; vmgco1, ventromedial type 1 glandular cell outlet; vmss, ventromedial sensory spot.

Fig. 14. Light micrographs showing trunk overview and detail in the head and neck of female holotype USNM 1558509 of *Echinoderes xalkutaat* sp. nov. (A) Overview of trunk, showing the lateral and ventral regions of the cuticular plates; (B) mouth cone, with detail of the outer oral styles; (C) introvert, with detail of a primary spinoscalid; (D) overview of introvert, showing the rings of regular scalids; (E) overview of neck, showing some ventral and lateral placids. Abbreviations: bs, basal sheath; bsf, basal

sheath's fringe; dp, distal end piece; mvp, midventral placid; oos, outer oral style; sc, scalid; tsp, trichoscalid plate.

Fig. 15. Light micrographs showing details of cuticular trunk characters of segments 1–5 of female holotype USNM 1558509 of *Echinoderes xalkutaat* sp. nov., with main focus on spines, tubes, sensory spots and glandular cell outlets. (A) Left half of ring plate of segment 1; (B) right half of ring plate of segment 1; (C) left half of ring plate of segment 2; (D) right half of ring plate of segment 2; (E) left half of tergal plate of segment 3; (F) right sternal plate of segment 3; (G) left half of tergal plate of segment 4; (H) right sternal plate of segment 4; (I) left half of tergal plate of segment 5; (J) right sternal plate of segment 5. Abbreviations: ldgco2, laterodorsal type 2 glandular cell outlet; ldss, laterodorsal sensory spot; lvt, lateroventral tube; mdgco1, middorsal type 1 glandular cell outlet; mds, middorsal spine; mdss, middorsal sensory spot; pgco1, paradorsal type 1 glandular cell outlet; sdgco2, subdorsal type 2 glandular cell outlet; sdss, subdorsal sensory spot; slgco2, sublateral type 2 glandular cell outlet; slss, sublateral sensory spot; vlgco2, ventrolateral type 2 glandular cell outlet; vlss, ventrolateral sensory spot; vmgco1, ventromedial type 1 glandular cell outlet; vmss, ventromedial sensory spot; sensory spots are marked as closed circles, and glandular cell outlets as dashed circles; numbers after abbreviation indicate the corresponding segment.

Fig. 16. Light micrographs showing details of cuticular trunk characters of segments 6–11 of female holotype USNM 1558509 of *Echinoderes xalkutaat* sp. nov., with main focus on spines, nephridiopores, sensory spots and glandular cell outlets. (A) Left half of tergal plate of segment 6; (B) right sternal plates of segments 6–8; (C) left half of tergal plate of segment 7; (D) left half of tergal plate of segment 8; (E) left half of tergal plate of segment 9; (F) right sternal plate of segment 9; (G) left half of tergal plates of segments 10–11; (H) right sternal plates of segments 10–11; (I) dorsal view of segment 11, with main focus on tergal extensions. Abbreviations: lane, lateral accessory nephridiopore; ldgco2, laterodorsal type 2 glandular cell outlet; ldss, laterodorsal sensory spot; lvs, lateroventral spine; mdgco1, middorsal type 1 glandular cell outlet; mds, middorsal spine; mlss, midlateral sensory spot; pdgco1, paradorsal type 1 glandular cell outlet; pdss, paradorsal sensory spot; sdss, subdorsal sensory spot; slgco2, sublateral type 2 glandular cell outlet; slss, sublateral sensory spot; te, tergal extension; vmgco1, ventromedial type 1 glandular cell outlet; vmss, ventromedial sensory spot;

1147 sensory spots are marked as closed circles, and glandular cell outlets as dashed circles;
1148 numbers after abbreviation indicate the corresponding segment.

1149

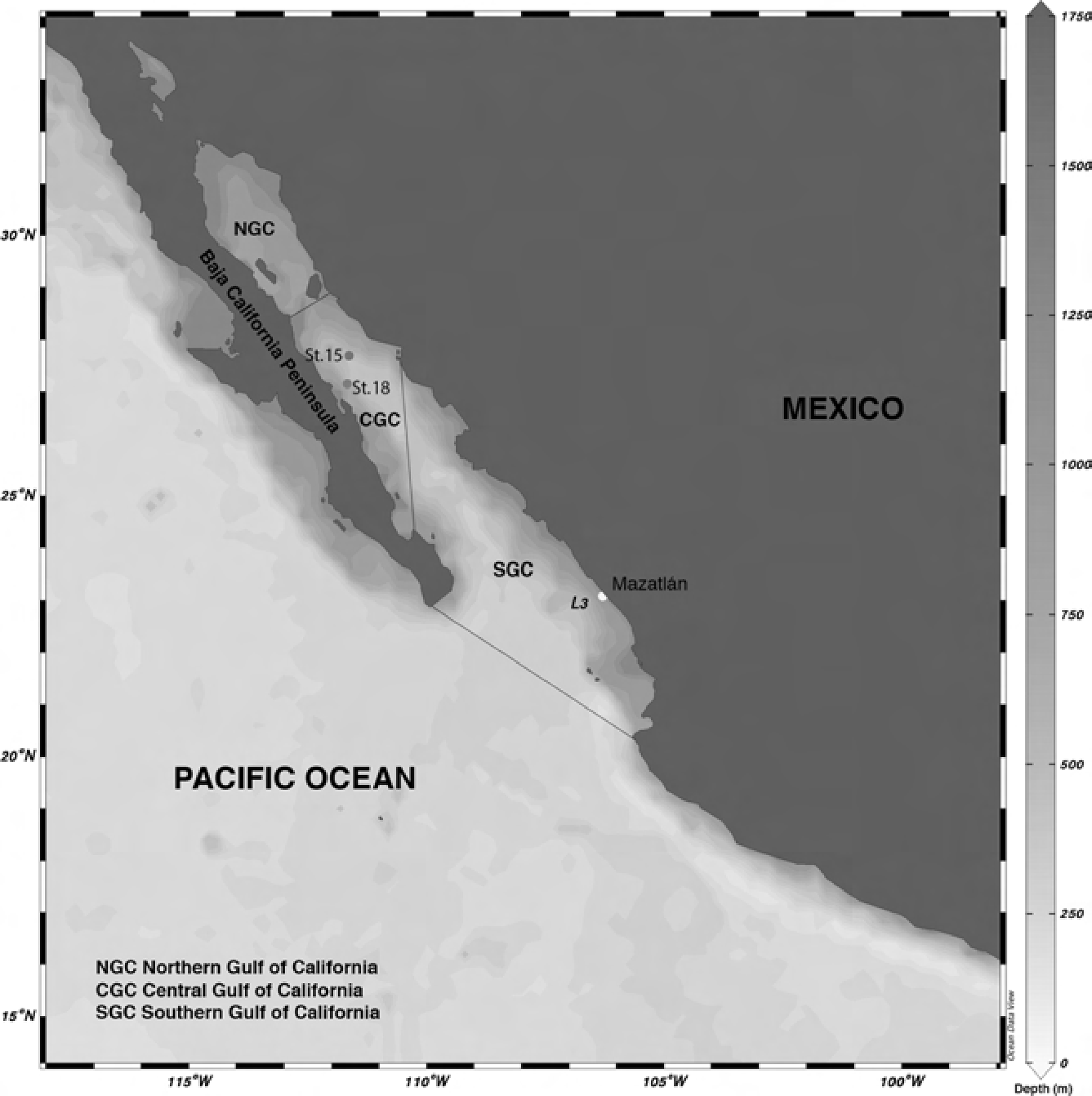
NGC
Baja California Peninsula
St.15
St.18
CGC
MEXICO
SGC
Mazatlán
L3
PACIFIC OCEAN
NGC Northern Gulf of California
CGC Central Gulf of California
SGC Southern Gulf of California
30°N
25°N
20°N
15°N
115°W
110°W
105°W
100°W
1750
1500
1250
1000
750
500
250
0
Depth (m)
Ocean Data View

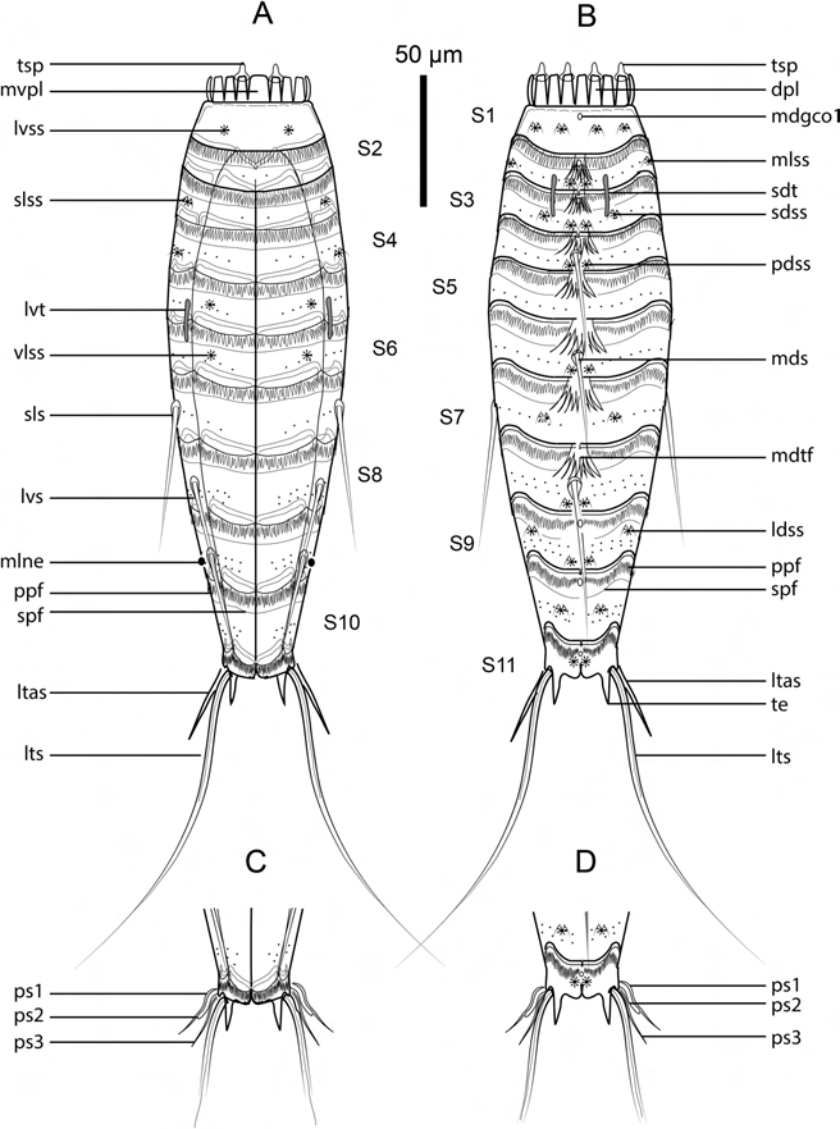
A
B
C
D
50 µm
tsp
mvpl
lvss
slss
lvt
vlss
sls
lvs
mlne
ppf
spf
ltas
lts
S2
S4
S6
S8
S10
dpl
mdgco1
mlss
sdt
sdss
pdss
mds
mdtf
ldss
S1
S3
S5
S7
S9
S11
te
ps1
ps2
ps3

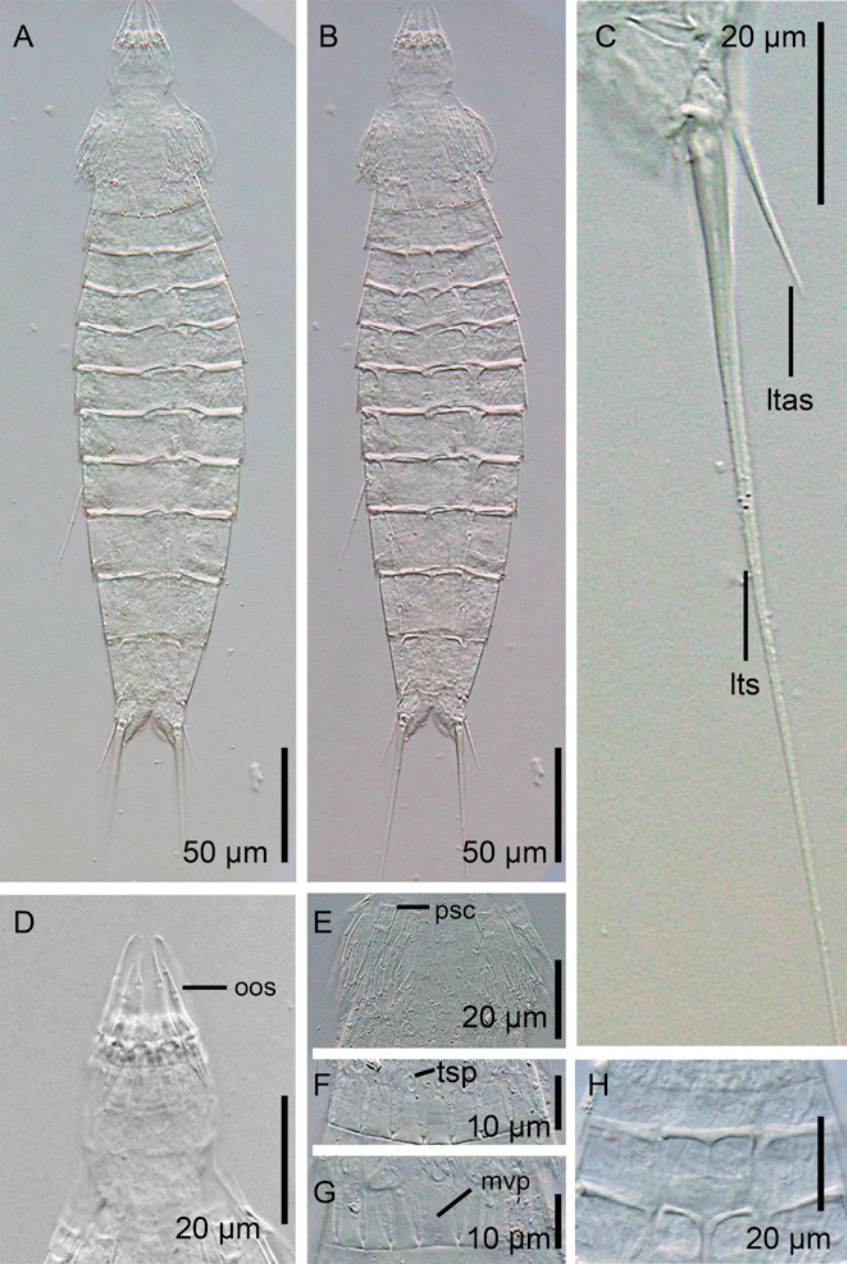
A
50 µm
B
50 µm
C
20 µm
ltas
lts
D
oos
20 µm
E
psc
20 µm
F
tsp
10 µm
G
mvp
10 µm
H
20 µm

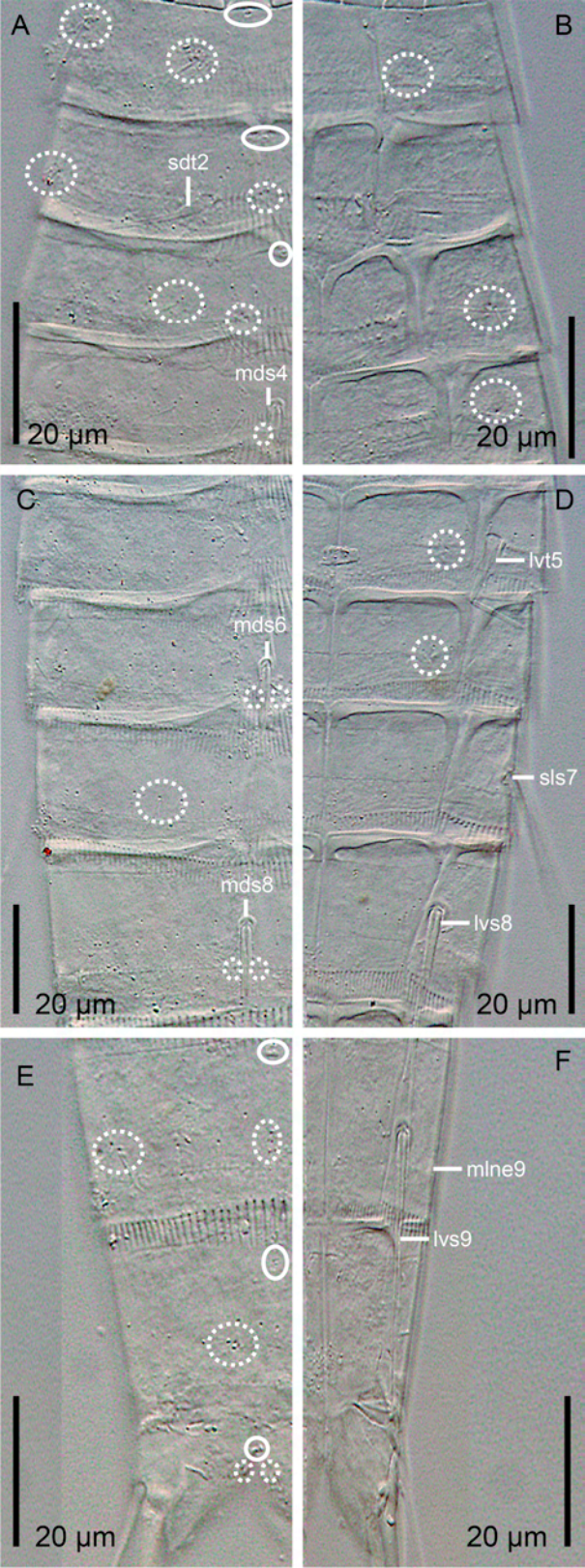
A
sdt2
mds4
20 µm
B
20 µm
C
mds6
mds8
20 µm
D
lvt5
sls7
lvs8
20 µm
E
20 µm
F
mlne9
lvs9
20 µm

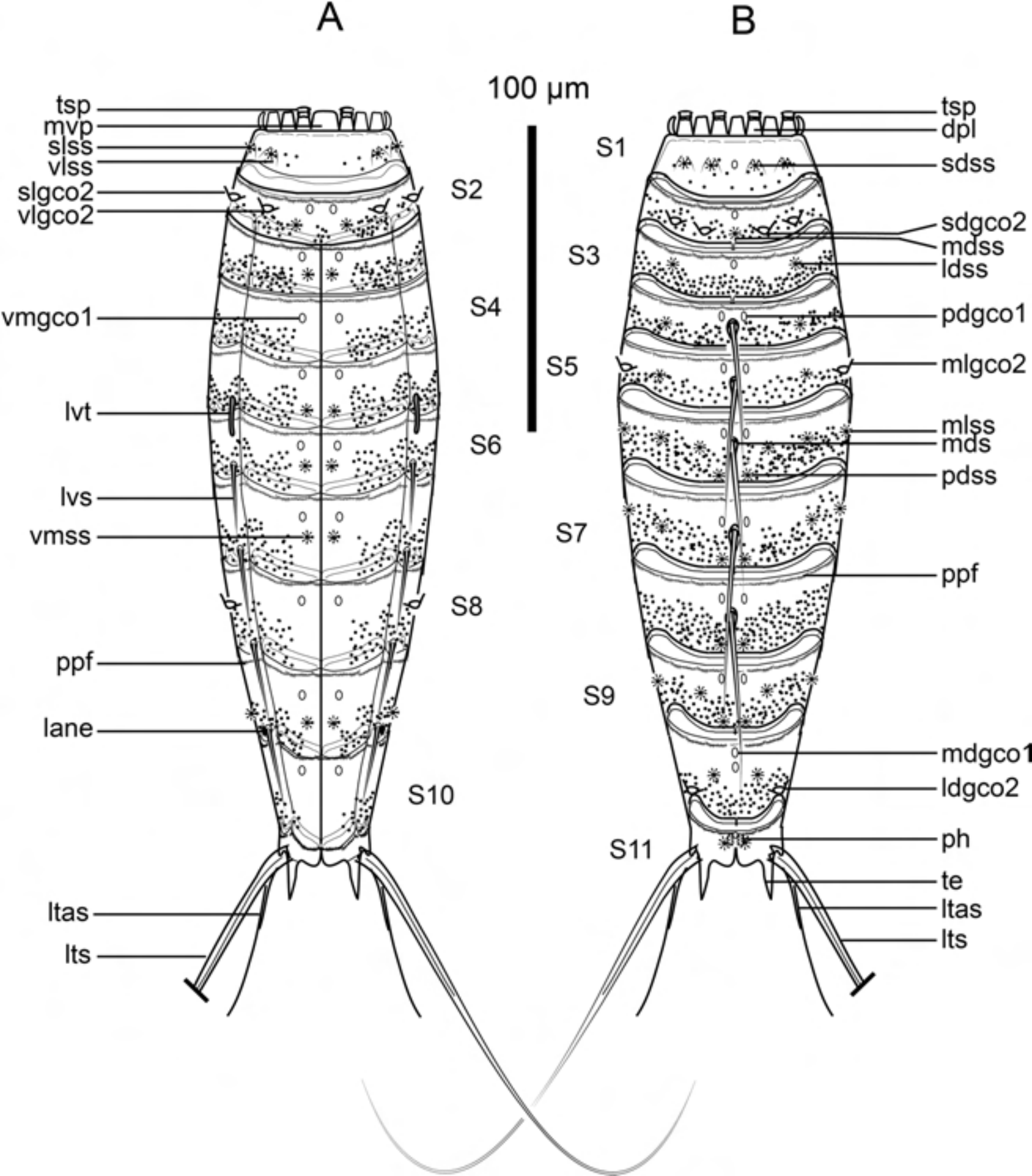
A
B
100 µm
tsp
mvp
slss
vlss
slgco2
vlgco2
vmgco1
lvt
lvs
vmss
ppf
lane
ltas
lts
S1
S2
S3
S4
S5
S6
S7
S8
S9
S10
S11
tsp
dpl
sdss
sdgco2
mdss
ldss
pdgco1
mlgco2
mlss
mds
pdss
ppf
mdgco1
ldgco2
ph
te
ltas
lts

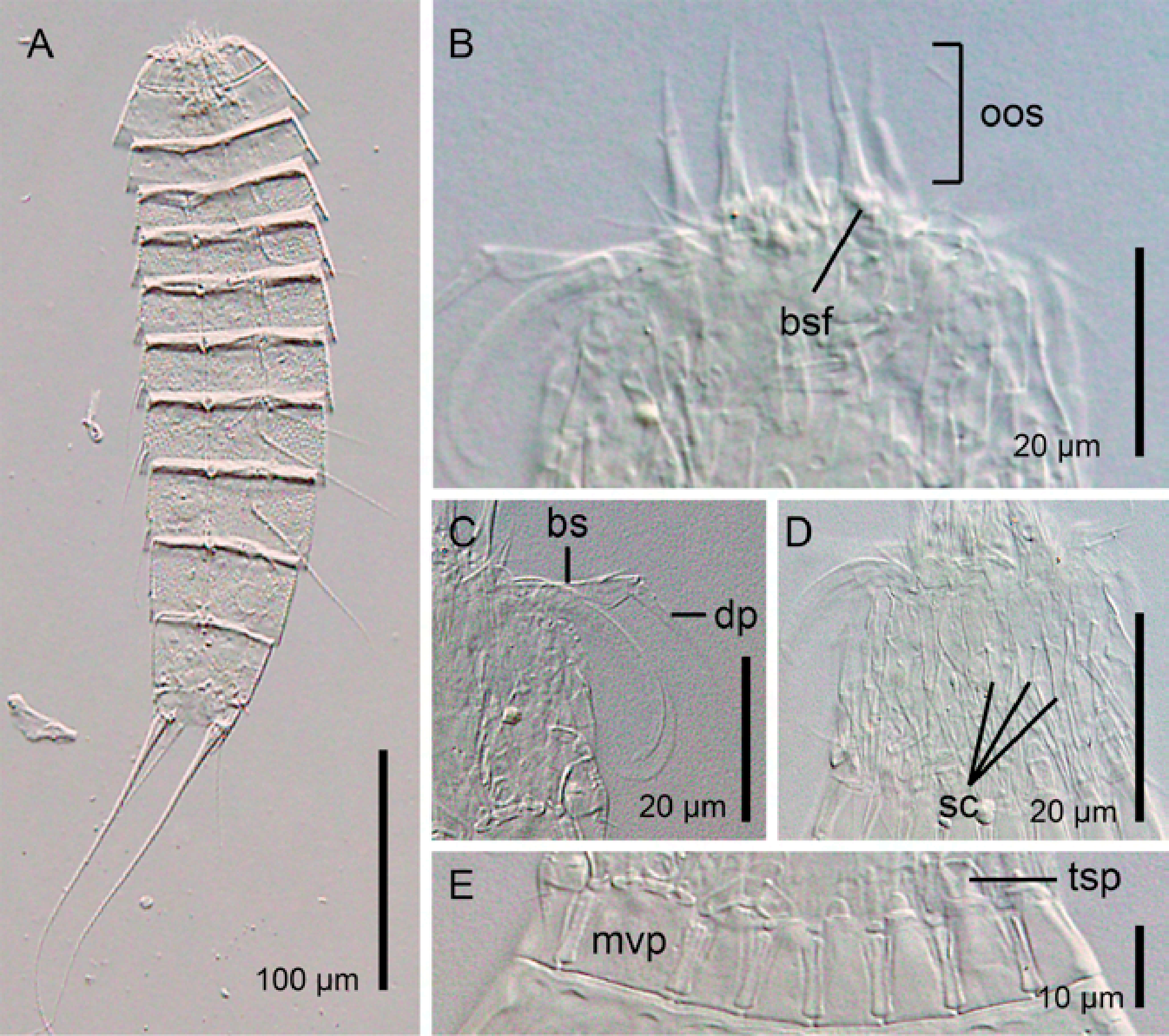
A
100 µm
B
oos
bsf
20 µm
C
bs
dp
20 µm
D
sc
20 µm
E
tsp
mvp
10 µm

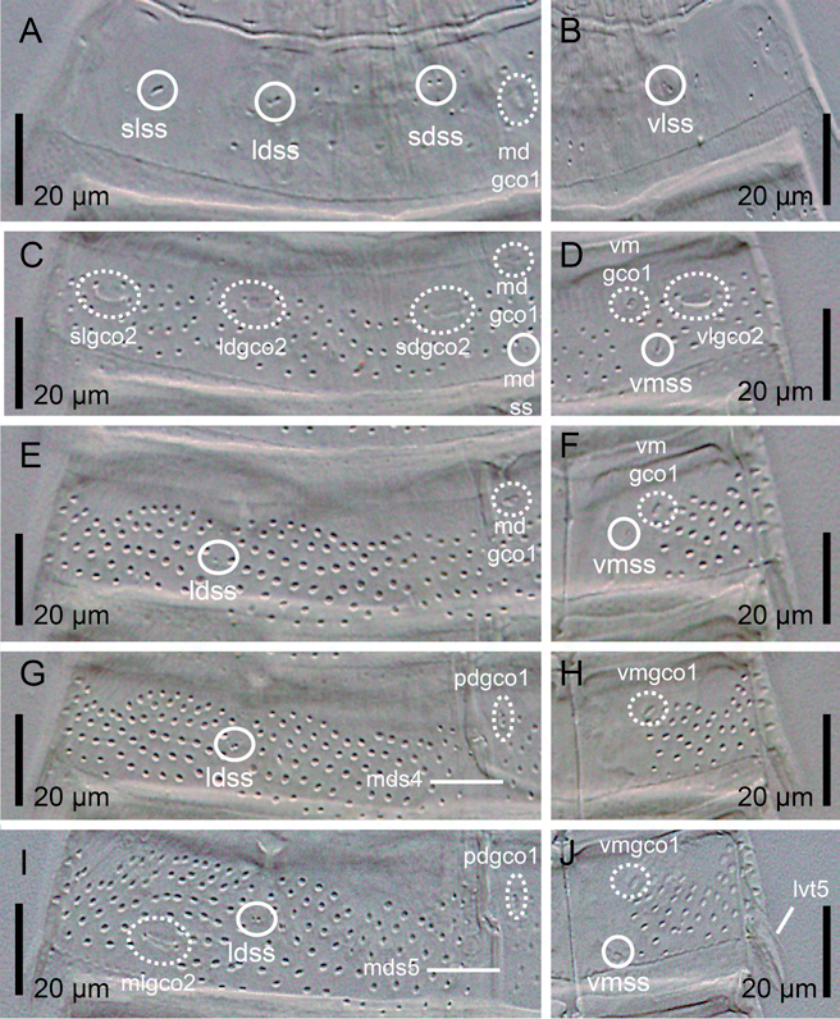
A
slss
ldss
sdss
md
gco1
20 µm
B
vlss
20 µm
C
slgco2
ldgco2
sdgco2
md
gco1
md
ss
20 µm
D
vm
gco1
vlgco2
vmss
20 µm
E
md
gco1
ldss
20 µm
F
vm
gco1
vmss
20 µm
G
pdgco1
ldss
mds4
20 µm
H
vmgco1
20 µm
I
pdgco1
ldss
mds5
migco2
20 µm
J
vmgco1
lvt5
vmss
20 µm

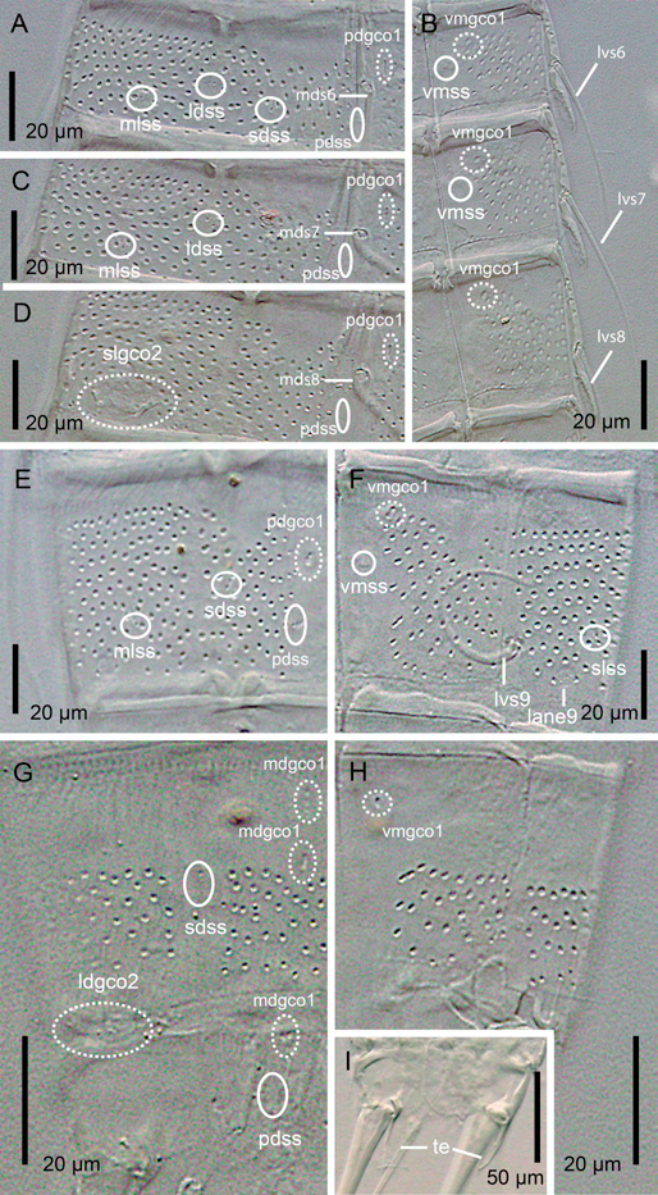
A
pdgco1
mlss
ldss
sdss
mds6
pdss
20 µm
B
vmgco1
lvs6
vmss
vmgco1
lvs7
vmss
vmgco1
lvs8
20 µm
C
pdgco1
mds7
ldss
mlss
pdss
20 µm
D
pdgco1
slgco2
mds8
pdss
20 µm
E
pdgco1
sdss
mlss
pdss
20 µm
F
vmgco1
vmss
slss
lvs9
lane9
20 µm
G
mdgco1
mdgco1
sdss
ldgco2
mdgco1
pdss
20 µm
H
vmgco1
I
te
50 µm
20 µm

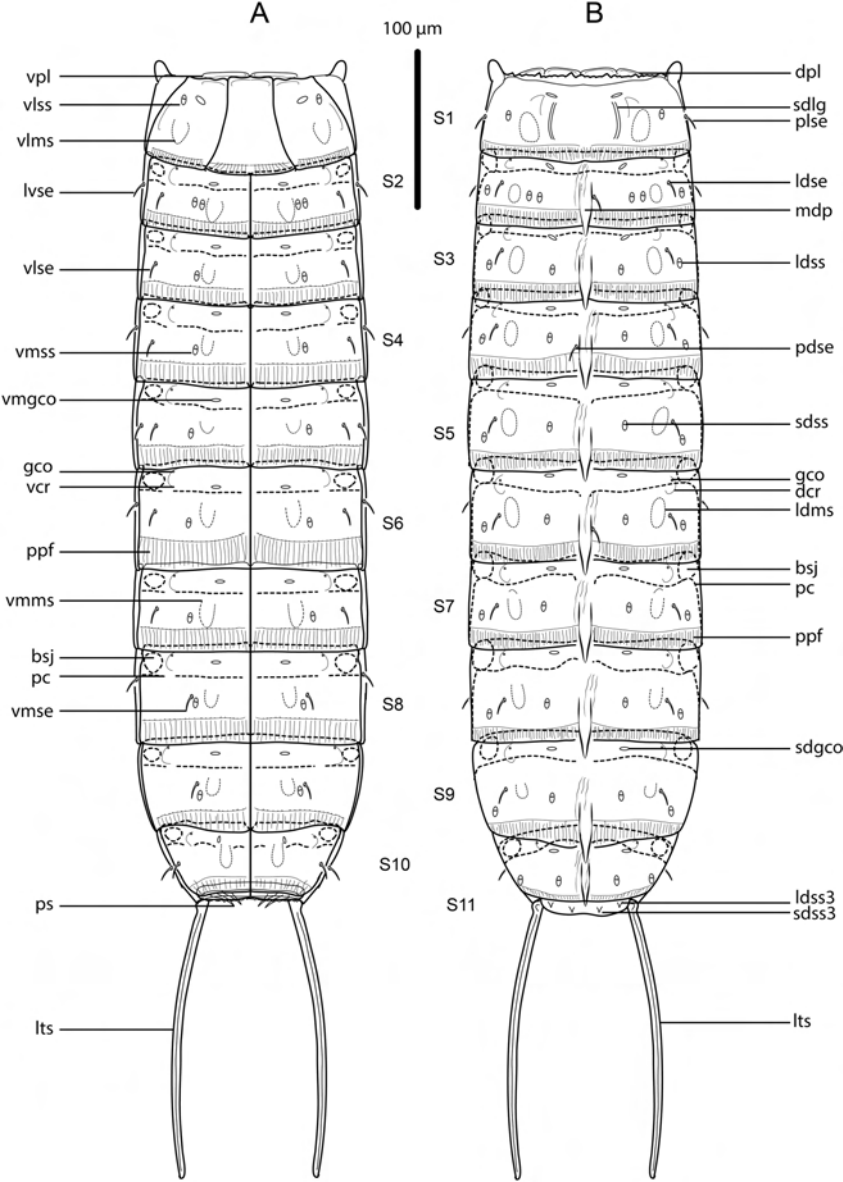
A
B
100 µm
vpl
vlss
vlms
lvse
vlse
vmss
vmgco
gco
vcr
ppf
vmms
bsj
pc
vmse
ps
lts
S1
S2
S3
S4
S5
S6
S7
S8
S9
S10
S11
dpl
sdlg
plse
ldse
mdp
ldss
pdse
sdss
gco
dcr
ldms
bsj
pc
ppf
sdgco
ldss3
sdss3
lts

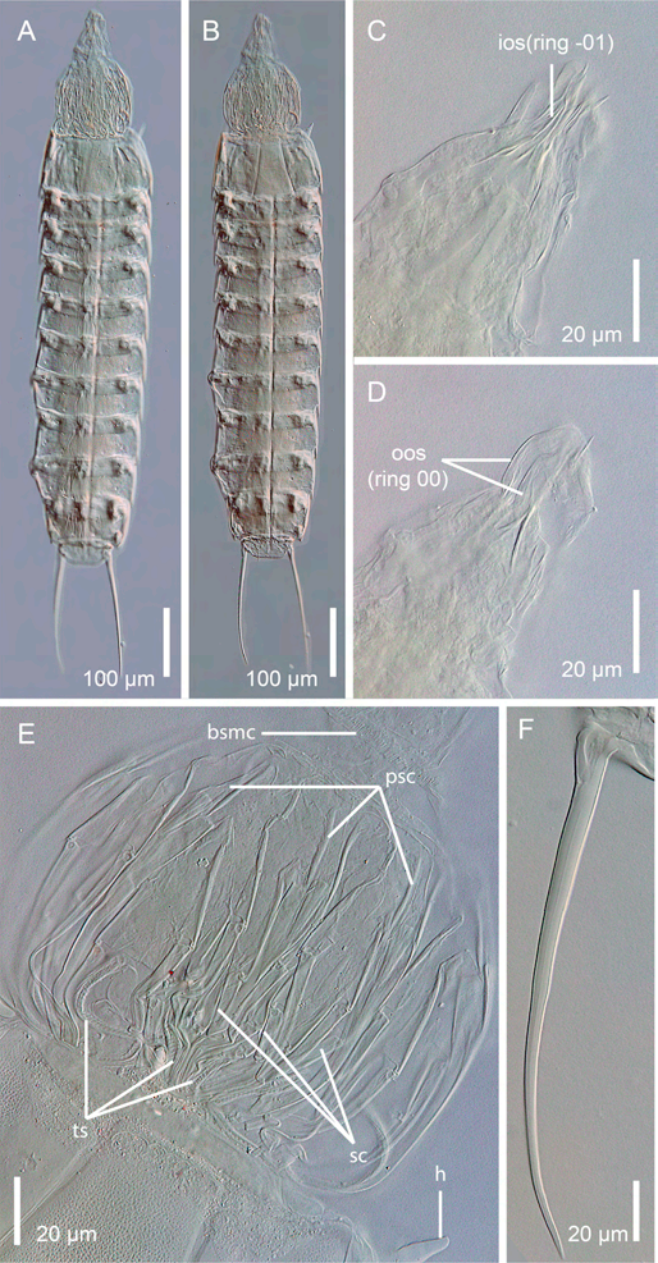
A
100 µm
B
100 µm
C
ios(ring -01)
20 µm
D
oos
(ring 00)
20 µm
E
bsmc
psc
ts
sc
h
20 µm
F
20 µm

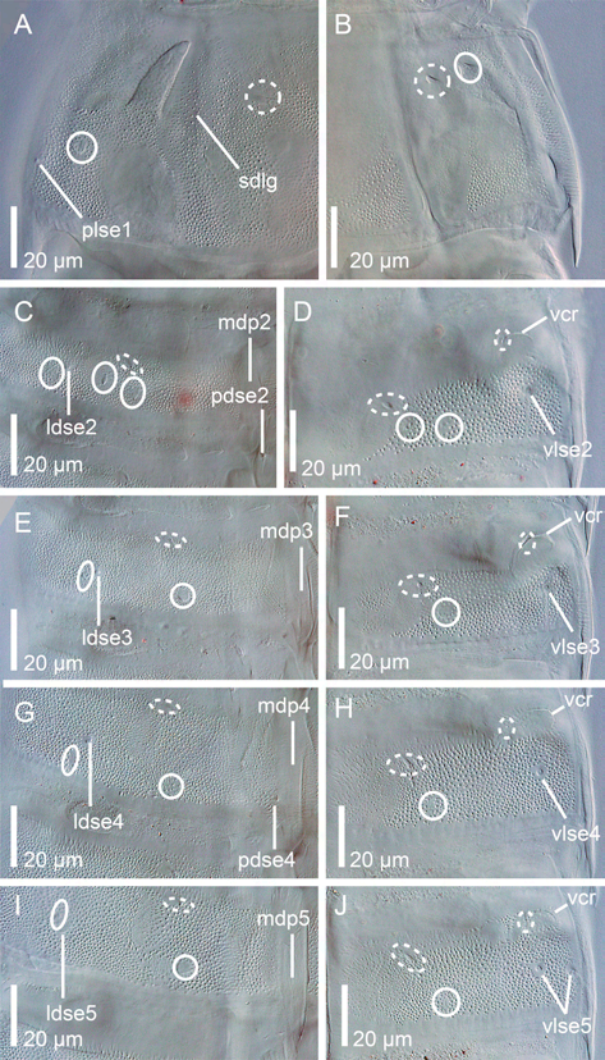
A
plse1
sdlg
20 µm
B
20 µm
C
mdp2
pdse2
ldse2
20 µm
D
vcr
vlse2
20 µm
E
mdp3
ldse3
20 µm
F
vcr
vlse3
20 µm
G
mdp4
ldse4
pdse4
20 µm
H
vcr
vlse4
20 µm
I
mdp5
ldse5
20 µm
J
vcr
vlse5
20 µm

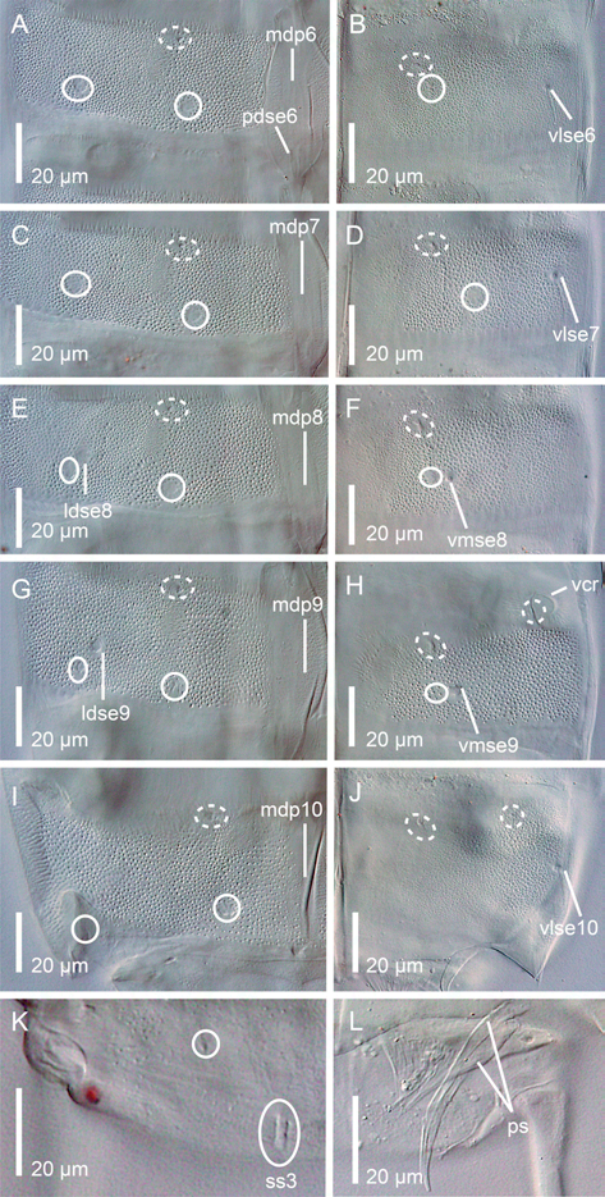
A
mdp6
pdse6
20 µm
B
vlse6
20 µm
C
mdp7
20 µm
D
vlse7
20 µm
E
mdp8
ldse8
20 µm
F
20 µm
vmse8
G
mdp9
ldse9
20 µm
H
vcr
20 µm
vmse9
I
mdp10
20 µm
J
vlse10
20 µm
K
20 µm
ss3
L
ps
20 µm

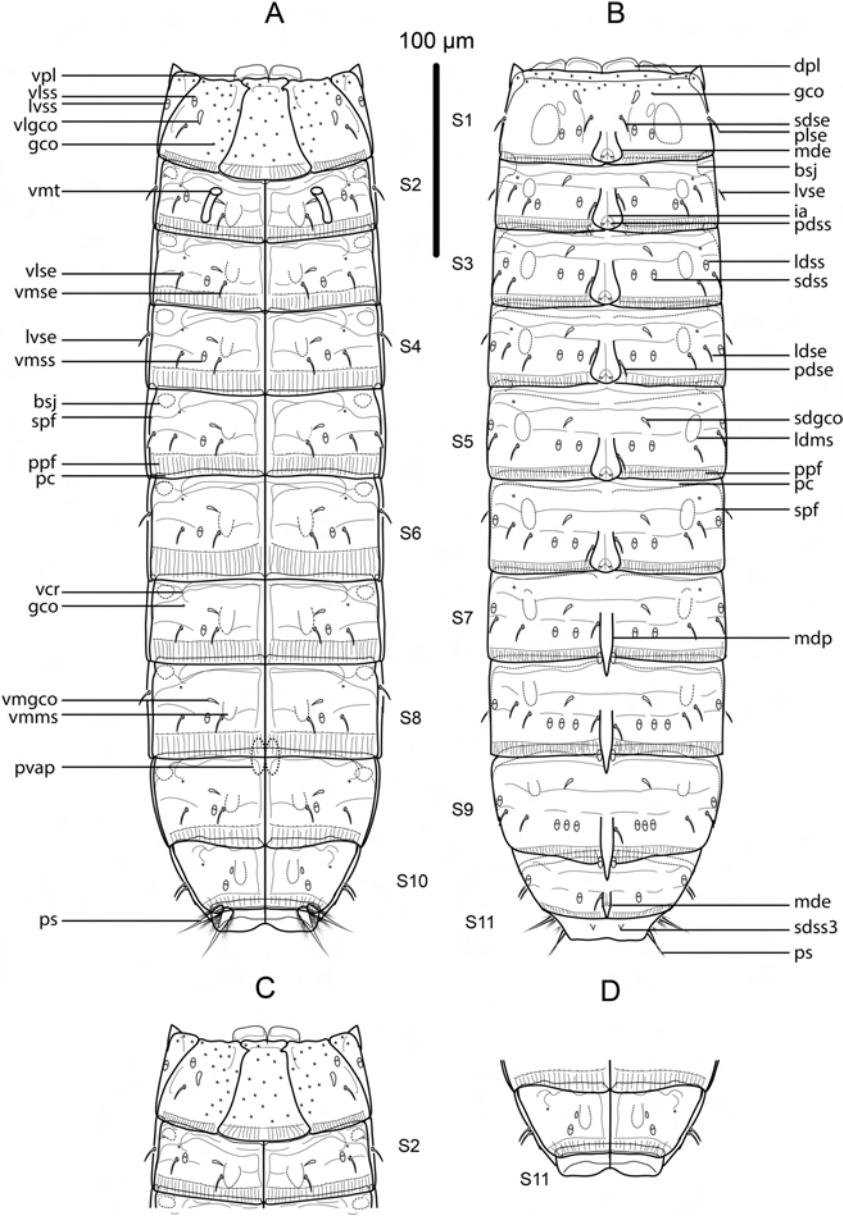
A
B
100 µm
vpl
vlss
lvss
vlgco
gco
vmt
vlse
vmse
lvse
vmss
bsj
spf
ppf
pc
vcr
gco
vmgco
vmms
pvap
ps
S1
S2
S3
S4
S5
S6
S7
S8
S9
S10
S11
dpl
gco
sdse
plse
mde
bsj
lvse
ia
pdss
ldss
sdss
ldse
pdse
sdgco
ldms
ppf
pc
spf
mdp
mde
sdss3
ps
C
D
S2
S11

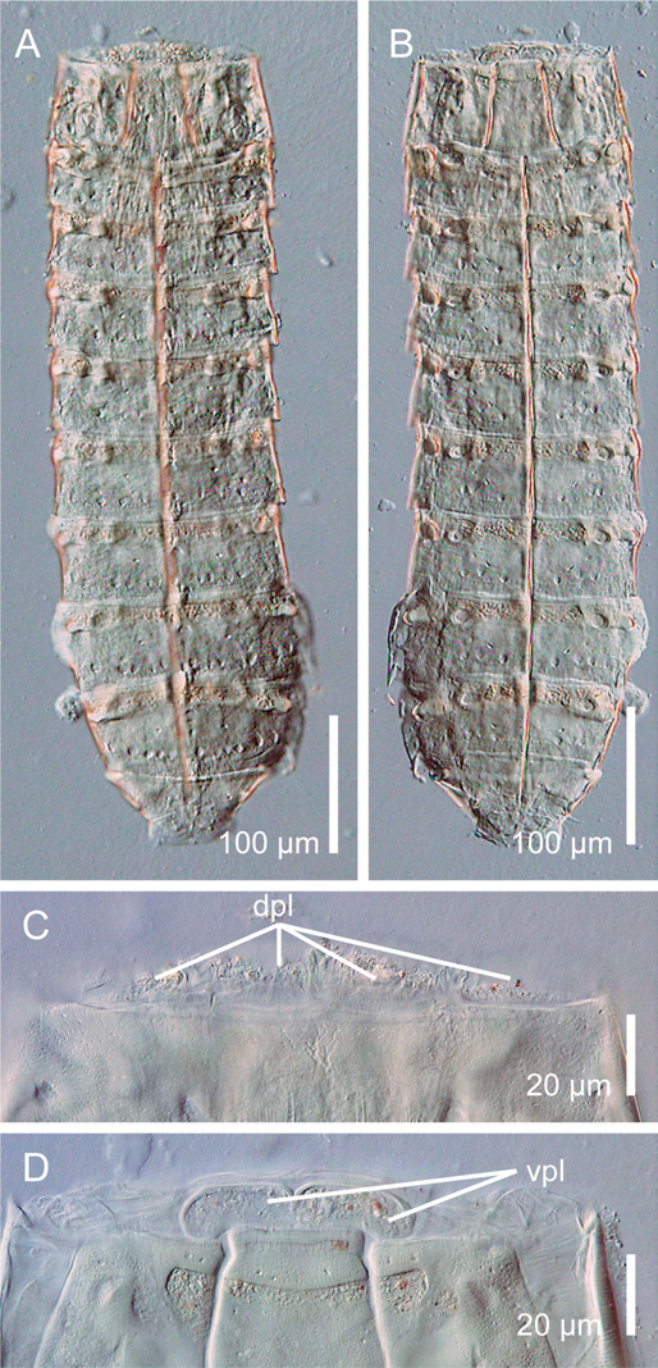
A
100 µm
B
100 µm
C
dpl
20 µm
D
vpl
20 µm

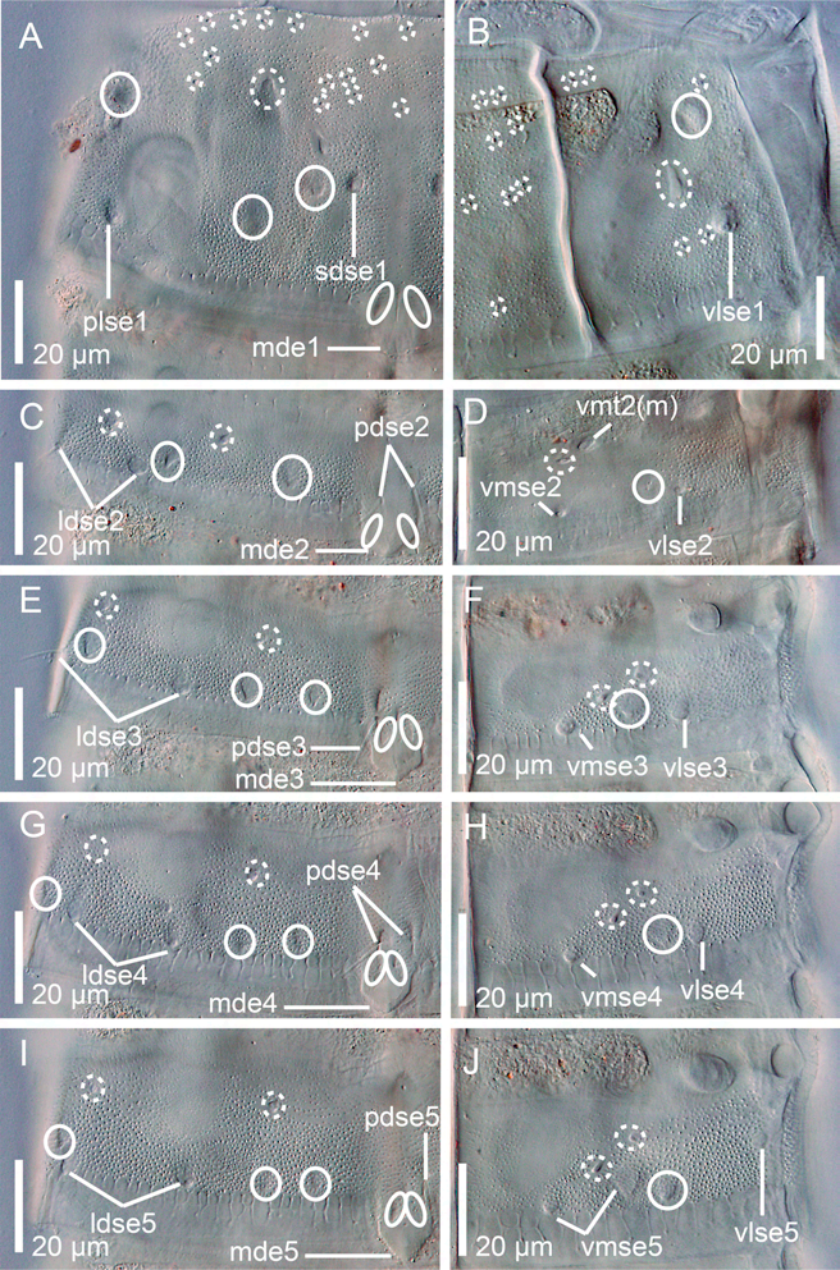
A
plse1
sdse1
mde1
20 µm
B
vlse1
20 µm
C
ldse2
pdse2
mde2
20 µm
D
vmt2(m)
vmse2
vlse2
20 µm
E
ldse3
pdse3
mde3
20 µm
F
vmse3
vlse3
20 µm
G
ldse4
pdse4
mde4
20 µm
H
vmse4
vlse4
20 µm
I
ldse5
pdse5
mde5
20 µm
J
vmse5
vlse5
20 µm

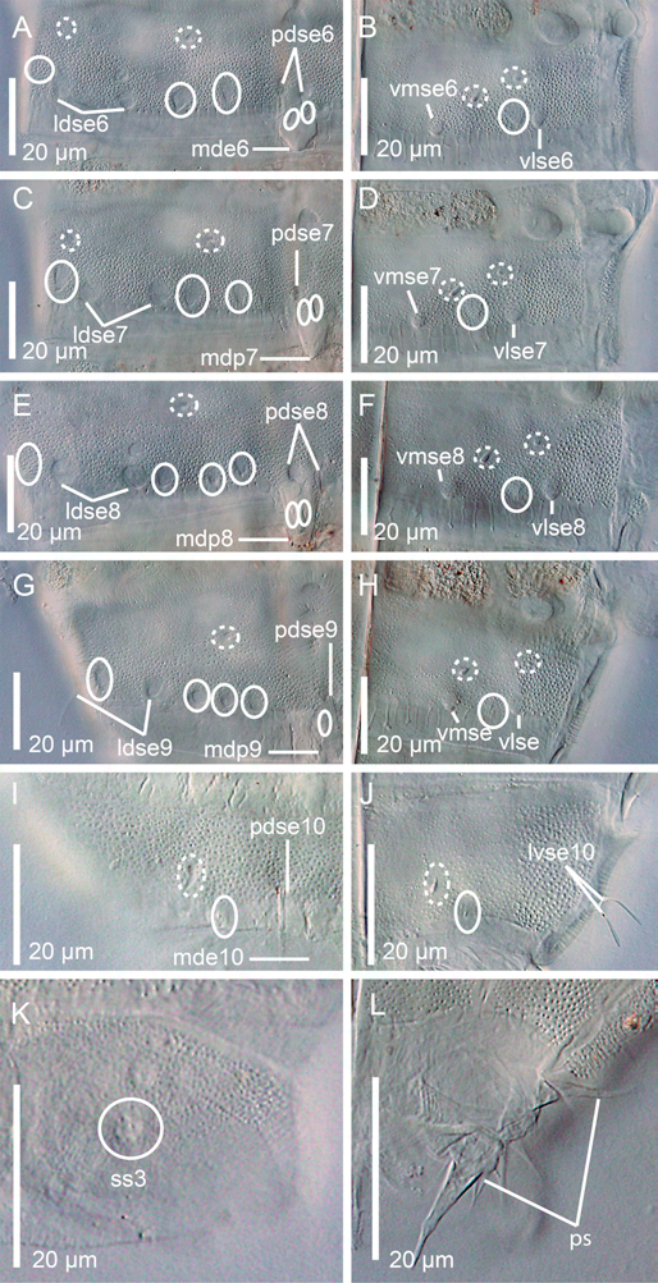
A
pdse6
ldse6
20 µm
mde6
B
vmse6
20 µm
vlse6
C
pdse7
ldse7
20 µm
mdp7
D
vmse7
20 µm
vlse7
E
pdse8
ldse8
20 µm
mdp8
F
vmse8
20 µm
vlse8
G
pdse9
20 µm
ldse9
mdp9
H
20 µm
vmse
vlse
I
pdse10
20 µm
mde10
J
lvse10
20 µm
K
ss3
20 µm
L
ps
20 µm